5

Spin–Orbit Coupling

This common body,
Like to a vagabond flag upon the stream,
Goes to and back, lackeying the varying tide,
To rot itself with motion.

William Shakespeare, *Anthony and Cleopatra, I, iv*

5.1 Introduction

In the last chapter, we considered the effect of tides raised on a satellite by a planet where we assumed that the satellite was in a synchronous spin state (i.e., that the rotational period of the satellite was equal to its orbital period). As mentioned in Sect. 1.6, most of the major natural satellites in the solar system are observed to be rotating in the synchronous state. How did this situation arise and what determines the spin–orbit state of a given satellite or planet? In this chapter, we start by further examining the effects of a tidal torque on a satellite's rotation. This analysis reveals why, for example, in order to maintain its synchronous spin–orbit resonance, the Moon must have a permanent quadrupole moment. The consequences of this extra torque on the system are then examined and this leads to a general approach to the concept of spin–orbit resonance in the solar system. The origin and stability of these resonances are also discussed.

5.2 Tidal Despinning

Consider the case of a satellite orbiting a planet in an elliptical orbit. Those parts of the orbit in which the satellite's spin rate, which we denote by $\dot{\eta} + n$, is less (or greater) than its angular velocity or the rate of change of its true anomaly $\dot{f}$, are shown in Fig. 5.1a. If we transform to a reference frame that is centred on the satellite and rotates with the satellite's mean motion n, then in this rotating frame the planet moves about its guiding centre in a 2:1 ellipse (cf. Sect. 4.5) as

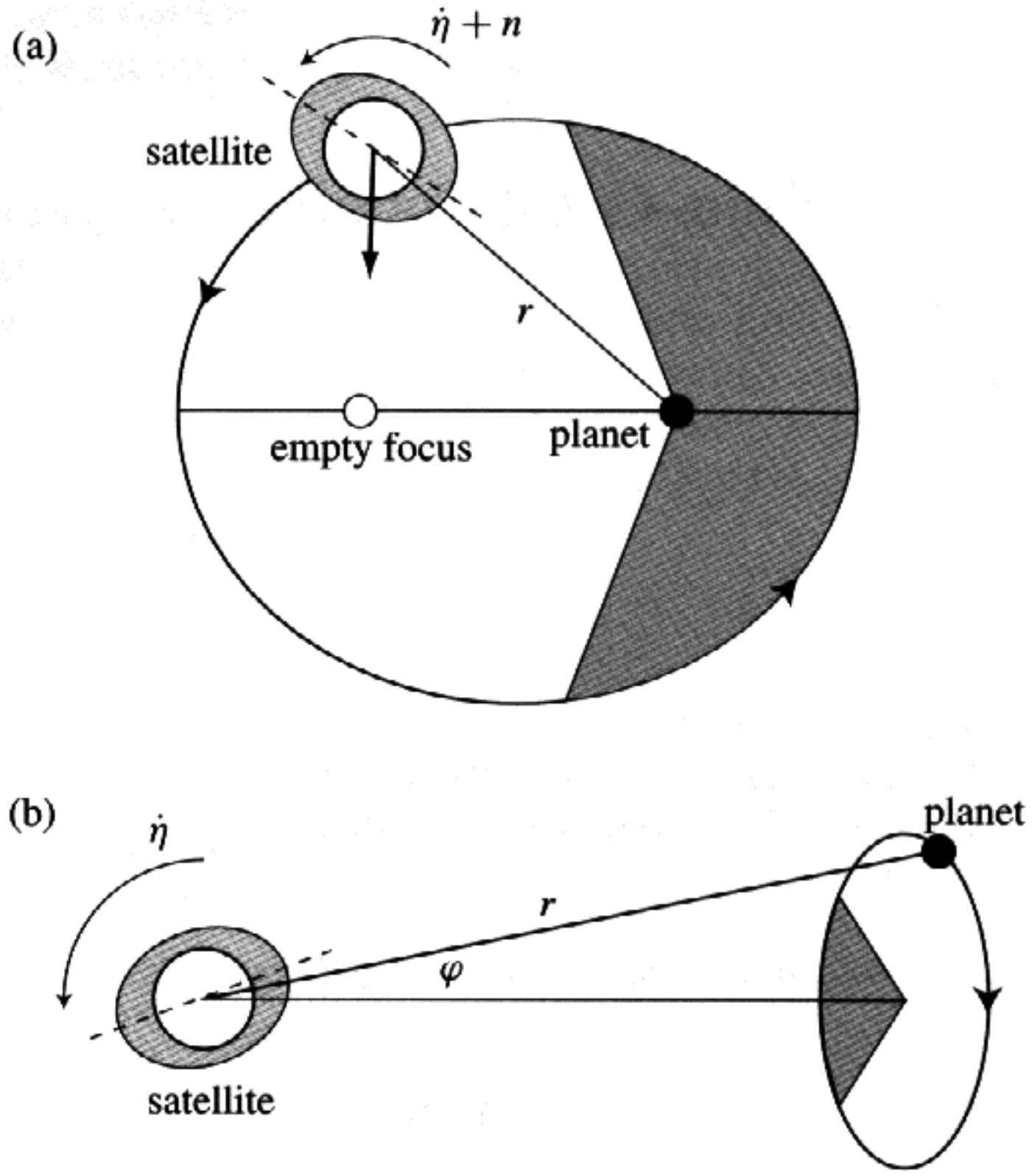

Fig. 5.1. (a) The path of a rotating satellite in an inertial reference frame centred on a planet. The nonshaded region shows that part of the orbit for which the spin rate of the satellite in inertial space, $\dot{\eta} + n > \dot{f}$. The dashed line denotes the axis of the tidal bulge. (b) The path of the planet in a reference frame centred on the satellite and rotating with its mean motion, n. The nonshaded region corresponds to the range of true anomaly for which $\dot{\eta} > \dot{\varphi}$.

shown in Fig. 5.1b. The rotation rate of the satellite in the rotating frame is $\dot{\eta}$ and the case $\langle \dot{\eta} \rangle = 0$ corresponds to the synchronous spin–orbit state.

For small values of the satellite's eccentricity e, the angle φ shown in Fig. 5.1b is given by

$$\varphi \approx 2e \sin nt. \tag{5.1}$$

Thus $\dot{\varphi}$ is a function of time and changes sign as the planet moves around the 2:1 ellipse. If $\dot{\eta} < 2en$, then when the satellite is close to pericentre, it is possible that $\dot{\varphi} > \dot{\eta}$. In Fig. 5.2a, the angular range over which, for some value of $\dot{\eta}$, this applies is denoted by the shaded area. In this region, the tide raised on the satellite by the planet lags behind the satellite–planet line (cf. Fig. 4.6) and a couple acts on the satellite to increase $\dot{\eta}$ and spin up the satellite (see Fig. 5.2a). In the unshaded region where $\dot{\varphi} < \dot{\eta}$, the situation is reversed and the tide raised

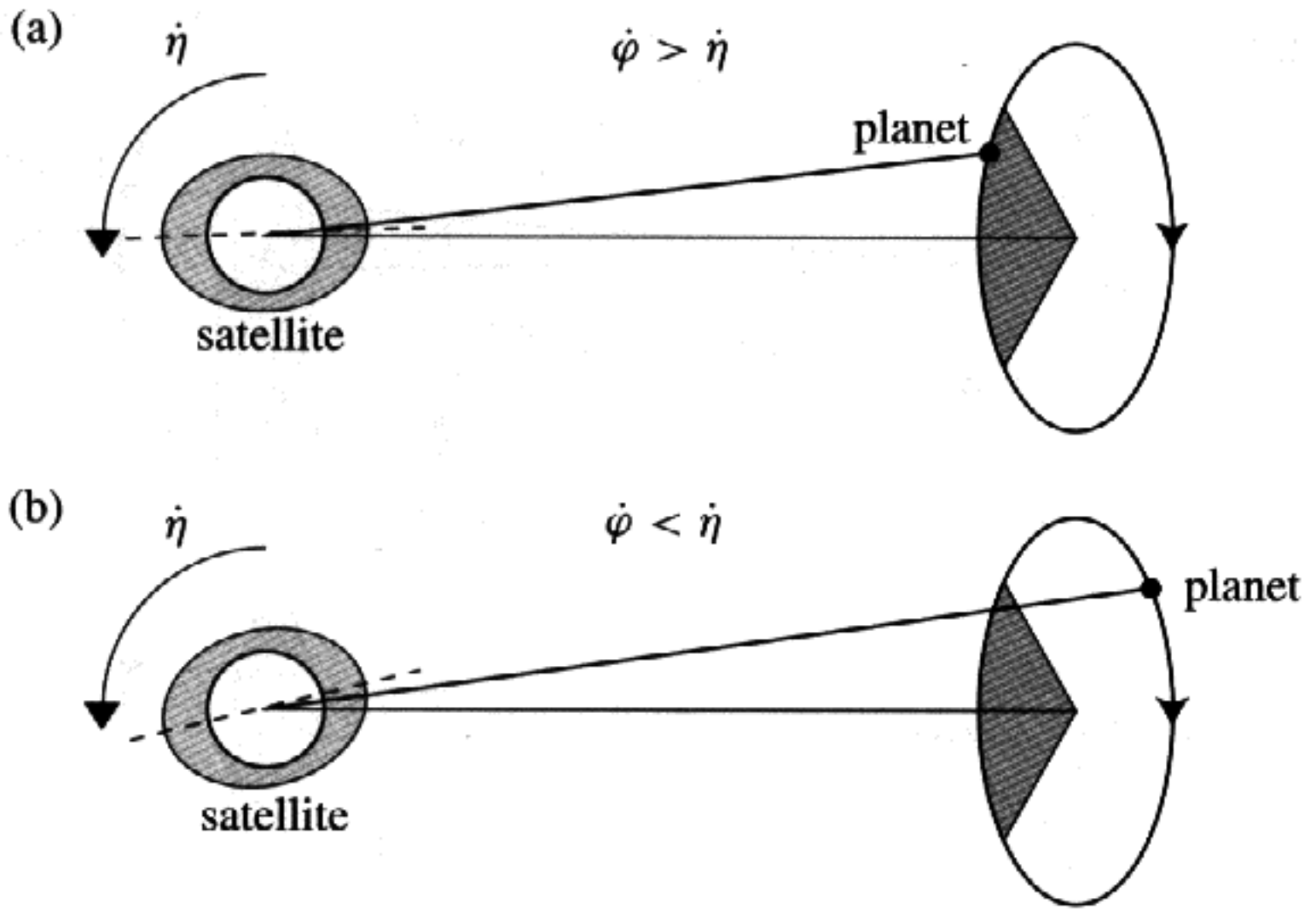

Fig. 5.2. (a) On the shaded part of orbit for which $\dot{\varphi} > \dot{\eta}$, the tide raised on the satellite by the planet lags behind the satellite–planet line (the dashed line denotes the axis of the tidal bulge) and a positive couple acts on the satellite to increase its spin rate. (b) On all other parts of the orbit, $\dot{\varphi} < \dot{\eta}$, the tidal bulge is carried ahead of the satellite–planet line and the spin of the satellite is braked.

on the satellite is carried ahead of the satellite–planet line (cf. Fig. 4.6). In this case, the resulting couple brakes the spin of the satellite and decreases $\dot{\eta}$ (see Fig. 5.2b):

By analogy with the situation examined in Sect. 4.3, the tidal torque acting to change the spin of the satellite is

$$N_s = -D\left(\frac{a}{r}\right)^6 \text{sign}\,(\dot{\eta} - \dot{\varphi}), \tag{5.2}$$

where

$$D = \frac{3}{2}\frac{k_2}{Q_s}\frac{n^4}{\mathcal{G}}R_s^5 \tag{5.3}$$

and is a positive constant, and Q_s, k_2, and R_s are the tidal dissipation function, Love number, and radius of the satellite, respectively. A positive torque will act to increase the spin of the satellite, $\dot{\eta}$. To find the mean torque, $\langle N_s \rangle$, we need to average N_s over one orbital period of the satellite. If we consider the special case where the satellite is in synchronous rotation ($\dot{\eta} = 0$), then the torque is positive on the near side of the centred ellipse and negative on the far side (see Fig. 5.3a). The planet spends equal intervals of time on each half of a 2:1 ellipse. However, since the radial distance is smaller on the near side, the mean torque is positive and will act to spin up the satellite. For equilibrium and zero mean torque, we must have $\dot{\eta} > 0$. In this case, the sign of the torque does not reverse

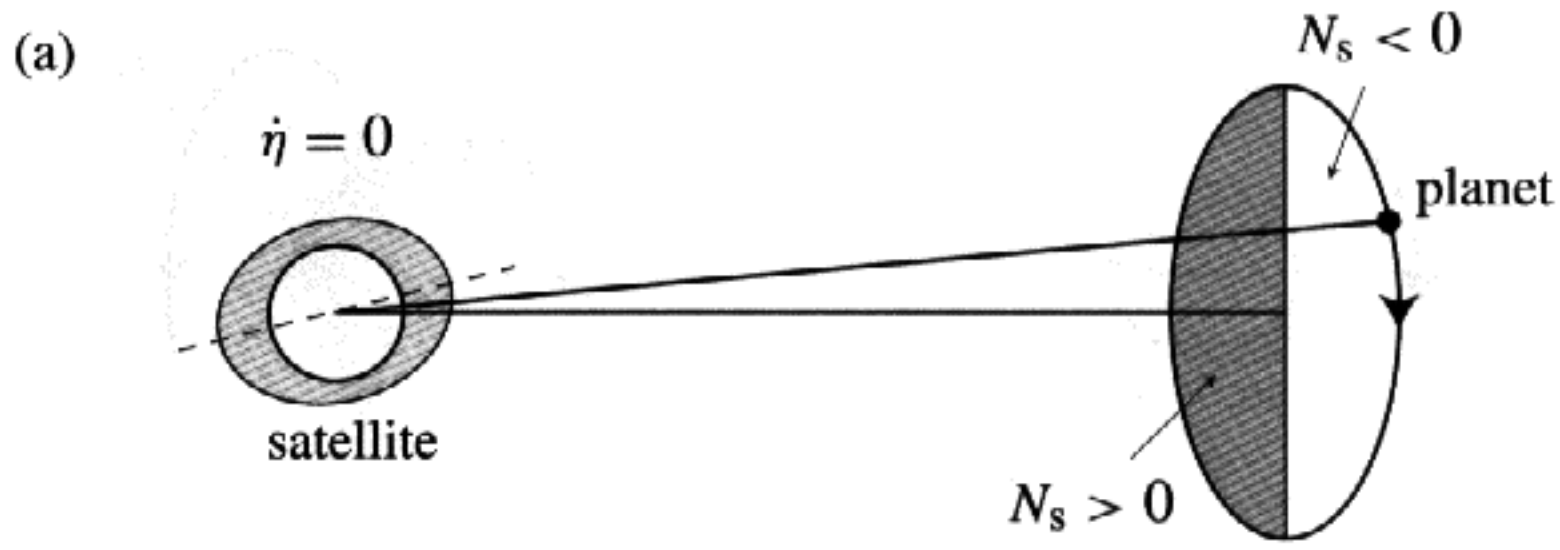

Fig. 5.3. (a) If $\dot{\eta} = 0$, then the tidal torque is positive and stronger on the near side of the planet's path and negative and weaker on the far side. Thus, the resultant net torque on the satellite is positive and the spin rate is increased. (b) In the equilibrium case, $\dot{\eta} > 0$ and the sign of the tidal torque on the satellite reverses closer to pericentre than apocentre. The stronger, positive torque (shaded area) now acts for less time than the weaker, negative torque.

at the midpoints of the 2:1 ellipse and equilibrium is achieved because the torque acting on the shaded part of the planet's path is stronger than that on the unshaded portion but acts for a shorter period of time (see Fig. 5.3b).

This argument suggests that the synchronous state is not stable and leads to a spinning up of the satellite. If this is the case, why are so many satellites observed to be in synchronous rotation? The answer is that other torques are acting, because, as in the case of the Moon, most satellites are at least partially solid and have permanent quadrupole moments, that is, permanent bulges or departures from sphericity. Before examining the effect of the quadrupole moment, we follow Goldreich (1966) and calculate the equilibrium spin rate in the absence of a permanent deformation.

The sign reversal in Eq. (5.2) occurs at those two points in orbit at which $\dot{\eta} = \dot{\varphi}$, or

$$\dot{f} = \dot{\eta} + n. \tag{5.4}$$

If $t = 0$ is the time of pericentre passage and sign reversal occurs when $t = \pm T$, then, since

$$f \approx nt + 2e \sin nt + \frac{5}{4} e^2 \sin 2nt, \tag{5.5}$$

sign reversal occurs when

$$\dot{\eta} = 2en \cos nT + \frac{5}{2} e^2 n \cos 2nT. \tag{5.6}$$

At the time of sign reversal, let

$$f = \pm\left(\frac{\pi}{2} - \delta\right). \tag{5.7}$$

Then

$$\sin\delta = \cos f = \cos(nT + 2e \sin nT) = \cos nT - 2e \sin^2 nT. \tag{5.8}$$

From Eq. (5.6),

$$\cos nT = \frac{\dot{\eta}}{2en} - \frac{5}{4} e \cos 2nT. \tag{5.9}$$

Hence, to $\mathcal{O}(e)$,

$$\sin\delta = \frac{\dot{\eta}}{2en} - \frac{5}{4}e + \frac{1}{2}e \sin^2 nT. \tag{5.10}$$

The mean tidal torque acting on the satellite is given by

$$\begin{aligned}\langle N_s \rangle &= -\frac{nD}{2\pi} \int_0^{2\pi/n} \left(\frac{a}{r}\right)^6 \operatorname{sign}(\dot{\eta} - \dot{\varphi})\, \mathrm{d}t \\ &= -\frac{D}{2\pi} \int_0^{2\pi} \left(\frac{a}{r}\right)^4 \frac{\operatorname{sign}(\dot{\eta} - \dot{\varphi})}{(1-e^2)^2}\, \mathrm{d}f.\end{aligned} \tag{5.11}$$

Allowing for the change of sign, this reduces to

$$\begin{aligned}\langle N_s \rangle &= +\frac{D}{\pi} \int_0^{(\pi/2)-\delta} (1 + 4e\cos f)\, \mathrm{d}f \\ &\quad - \frac{D}{\pi} \int_{(\pi/2)-\delta}^{\pi} (1 + 4e\cos f)\, \mathrm{d}f \\ &= +\frac{2D}{\pi}(4e\cos\delta - \delta).\end{aligned} \tag{5.12}$$

For equilibrium, we must have $\langle N_s \rangle = 0$ and this requires that

$$\delta = 4e\cos\delta \approx 4e\left(1 - \frac{1}{2}\delta^2\right) \approx 4e. \tag{5.13}$$

It follows from this and Eqs. (5.5) and (5.7) that we have the relationship

$$\begin{aligned}\sin nT &\approx \sin f \approx \sin[\pm(\pi/2 - \delta)] \\ &= \cos\delta \approx \cos 4e \approx 1 - 8e^2 \\ &\approx 1.\end{aligned}$$

Substituting into Eq. (5.10), we obtain the result

$$\dot{\eta} = \frac{19}{2} e^2 n. \tag{5.14}$$

Thus, in the absence of a permanent quadrupole moment, the Moon, for example, would rotate about 3% faster than the observed synchronous rate, and over a period of about 2.6 y, we would see both sides of the satellite.

Before closing this introductory section, we need to emphasize that in Eq. (5.2) we formulated the effects of tidal drag using the model due to MacDonald (1964) that assumes a constant lag angle for the tidal bulge. If we had chosen to use the alternative formulation of Darwin (1908) in which the tidal potential is expanded in a Fourier time series and each component of the tide is given a constant phase lag, then our conclusions would be substantially different. Goldreich & Peale (1966) discuss this in detail.

5.3 The Permanent Quadrupole Moment

To calculate the external gravitational field of a permanently deformed satellite at any distance from its centre of mass, we require a description of the distribution of mass within the satellite. At very large distances, the field is well represented by that of a point mass. At lesser, but still large, distances, the information on the mass distribution provided by the satellite's principal moments of inertia proves to be sufficient. The derivations that follow are based chiefly on those given by MacMillan (1936) and Ramsey (1937, 1940).

Consider an element of mass at a point P within a body and let the position vector of this element with respect to an arbitrary origin at O be $\mathbf{p} = (x, y, z)$ (see Fig. 5.4). We define the following moments of inertia with respect to the coordinate axes:

$$\mathcal{A} = \sum \delta m(y^2 + z^2), \tag{5.15}$$

$$\mathcal{B} = \sum \delta m(z^2 + x^2), \tag{5.16}$$

$$\mathcal{C} = \sum \delta m(x^2 + y^2) \tag{5.17}$$

and the following products of inertia

$$\mathcal{D} = \sum \delta m\, yz, \tag{5.18}$$

$$\mathcal{E} = \sum \delta m\, zx, \tag{5.19}$$

$$\mathcal{F} = \sum \delta m\, xy. \tag{5.20}$$

The moment of inertia I_L about any line OL can be expressed in terms of $\mathcal{A}$, $\mathcal{B}, \mathcal{C}, \mathcal{D}, \mathcal{E}$, and $\mathcal{F}$ and the direction cosines l, m, and n of the line OL with respect to the x, y, and z axes. Let PQ be the perpendicular from the point $P(x, y, z)$ to the line OL, where the position vector of Q is given by $\mathbf{q} = (x', y', z')$. Hence $OP = p$ and $OQ = q$, the magnitudes of the vectors $\mathbf{p}$ and $\mathbf{q}$. Because PQ is perpendicular to OL, we have

$$\mathbf{p} \cdot \mathbf{q} = q^2. \tag{5.21}$$

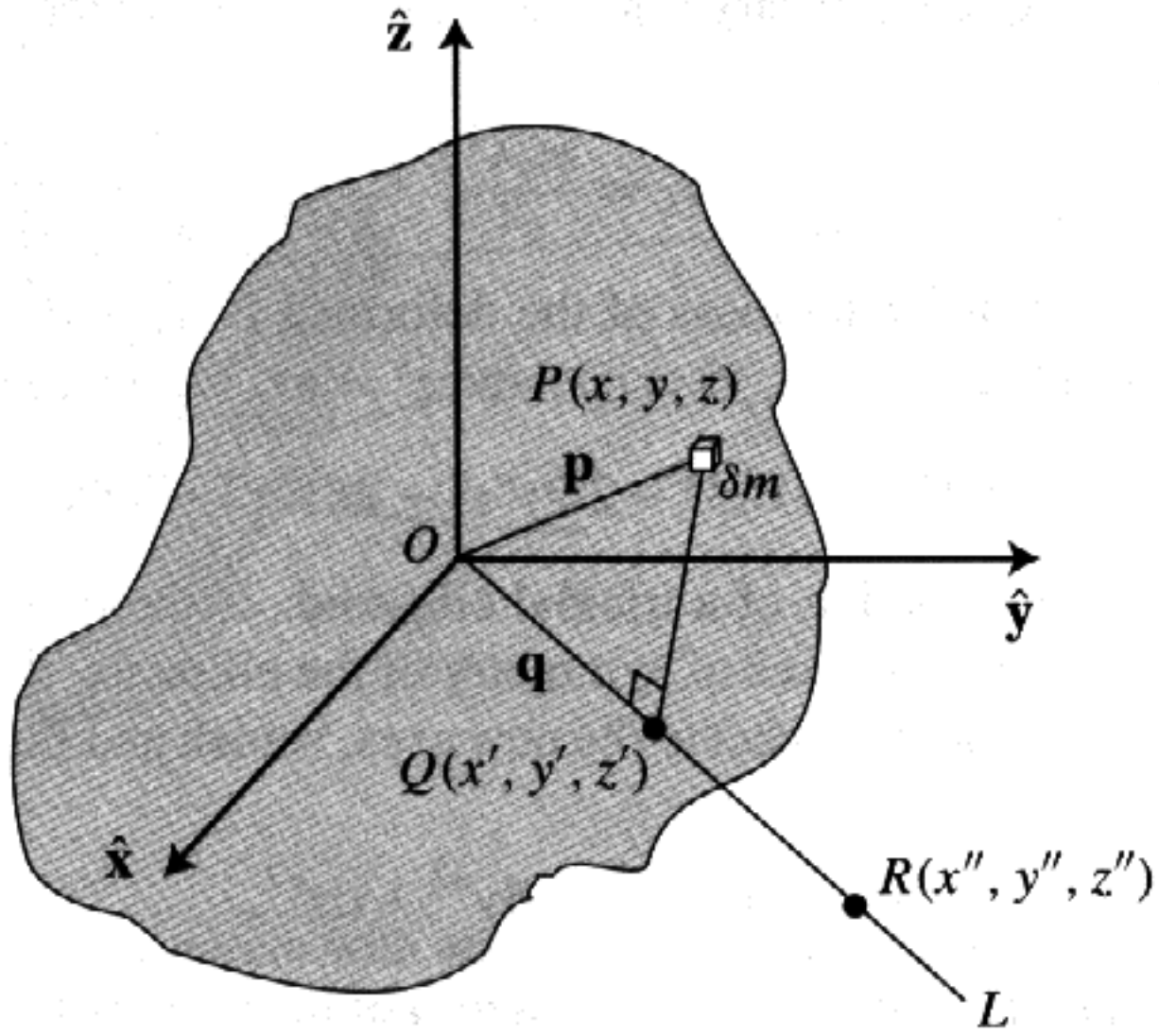

Fig. 5.4. The location of a mass element δm at a point P within the body with position vector $\mathbf{p} = (x, y, z)$. OL is an arbitrary line from the origin of the coordinate system at O. PQ is the perpendicular from P to the point Q with position vector $\mathbf{q} = (x', y', z')$ along the line OL. The arbitrary point R with position vector $\mathbf{r} = (x'', y'', z'')$ also lies along the line OL.

However,

$$\mathbf{p} \cdot \mathbf{q} = xx' + yy' + zz' = x(lq) + y(mq) + z(nq) = q(lx + my + nz) \qquad (5.22)$$

and hence

$$q = lx + my + nz. \qquad (5.23)$$

The moment of inertia I_L is given by

$$I_L = \sum \delta m (PQ)^2 = \sum \delta m \left[x^2 + y^2 + z^2 - (lx + my + nz)^2 \right]. \qquad (5.24)$$

Because $l^2 + m^2 + n^2 = 1$, we can write

$$I_L = \sum \delta m \left[(x^2 + y^2 + z^2)(l^2 + m^2 + n^2) - (lx + my + nz)^2 \right], \qquad (5.25)$$

which, on expanding and rearranging, gives

$$\begin{aligned} I_L = {} & l^2 \sum \delta m (y^2 + z^2) + m^2 \sum \delta m (z^2 + x^2) + n^2 \sum \delta m (x^2 + y^2) \\ & - 2mn \sum \delta m \, yz - 2nl \sum \delta m \, zx - 2lm \sum \delta m \, xy. \end{aligned} \qquad (5.26)$$

This can be written as

$$I_L = \mathcal{A}l^2 + \mathcal{B}m^2 + \mathcal{C}n^2 - 2\mathcal{D}mn - 2\mathcal{E}nl - 2\mathcal{F}lm. \qquad (5.27)$$

If we now consider an arbitrary point $R(x'', y'', z'')$ a distance r from O on the line OL and write

$$I_L = \frac{m_s \lambda^4}{r^2}, \tag{5.28}$$

where $m_s = \sum \delta m$ is the total mass of the deformed body and λ is an arbitrary length, then, given that $x'' = lr$, $y'' = mr$, and $z'' = nr$, Eq. (5.27) becomes

$$m_s \lambda^4 = \mathcal{A}x''^2 + \mathcal{B}y''^2 + \mathcal{C}z''^2 - 2\mathcal{D}y''z'' - 2\mathcal{E}z''x'' - 2\mathcal{F}x''y'', \tag{5.29}$$

which is the general equation of a triaxial ellipsoid. If the coordinate axes are chosen to coincide with the axes of symmetry of the ellipsoid, then the products of inertia $\mathcal{D}$, $\mathcal{E}$, and $\mathcal{F}$, with respect to the new axes, vanish and Eq. (5.29) reduces to

$$m_s \lambda^4 = \mathcal{A}x''^2 + \mathcal{B}y''^2 + \mathcal{C}z''^2. \tag{5.30}$$

These new axes are the principal axes of inertia of the body defined with respect to the point O. Equation (5.30) defines the *ellipsoid of inertia* (see Cauchy (1827) for details of the above calculation). This is an invariant of the body; it is independent of the orientation of the axes but varies with the position of the origin O. If O is the centre of mass, then the ellipsoid is called the *central ellipsoid of inertia.* It follows from the properties of this ellipsoid that every body, regardless of its shape, possesses three mutually perpendicular axes, such that the moment of inertia about one of these axes is a maximum, while another is a minimum and the third is either intermediate or equal to one of the other two.

We now derive an expression for the external gravitational field of a permanently deformed satellite in terms of its principal moments of inertia, $\mathcal{A}$, $\mathcal{B}$, and $\mathcal{C}$ defined with respect to the centre of mass. In our new system (see Fig. 5.5), we take the point O to be at the centre of mass of the satellite and let P be a point a distance r from O. We will assume that r is very much greater than the mean radius of the satellite. Let the coordinate system be defined such that the x, y, and z directions lie along the principal axes of inertia of the satellite (see Fig. 5.5).

If δm is the mass of a small mass element at the point Q, distance R from O, then the potential of the satellite at P is given by

$$V = -\sum \frac{\mathcal{G}\delta m}{\Delta} = -\sum \frac{\mathcal{G}\delta m}{(r^2 + R^2 - 2rR\cos\theta)^{1/2}}, \tag{5.31}$$

where θ is the angle between OP and OQ and the summation is taken over all mass elements. Expanding Eq. (5.31) binomially and neglecting high-order terms ($r \gg R$ for all Q), we obtain

$$V \approx -\frac{\mathcal{G}m_s}{r} - \frac{\sum \mathcal{G}\delta m R\cos\theta}{r^2} - \frac{2\sum \mathcal{G}\delta m R^2 - 3\sum \mathcal{G}\delta m R^2 \sin^2\theta}{2r^3}, \tag{5.32}$$

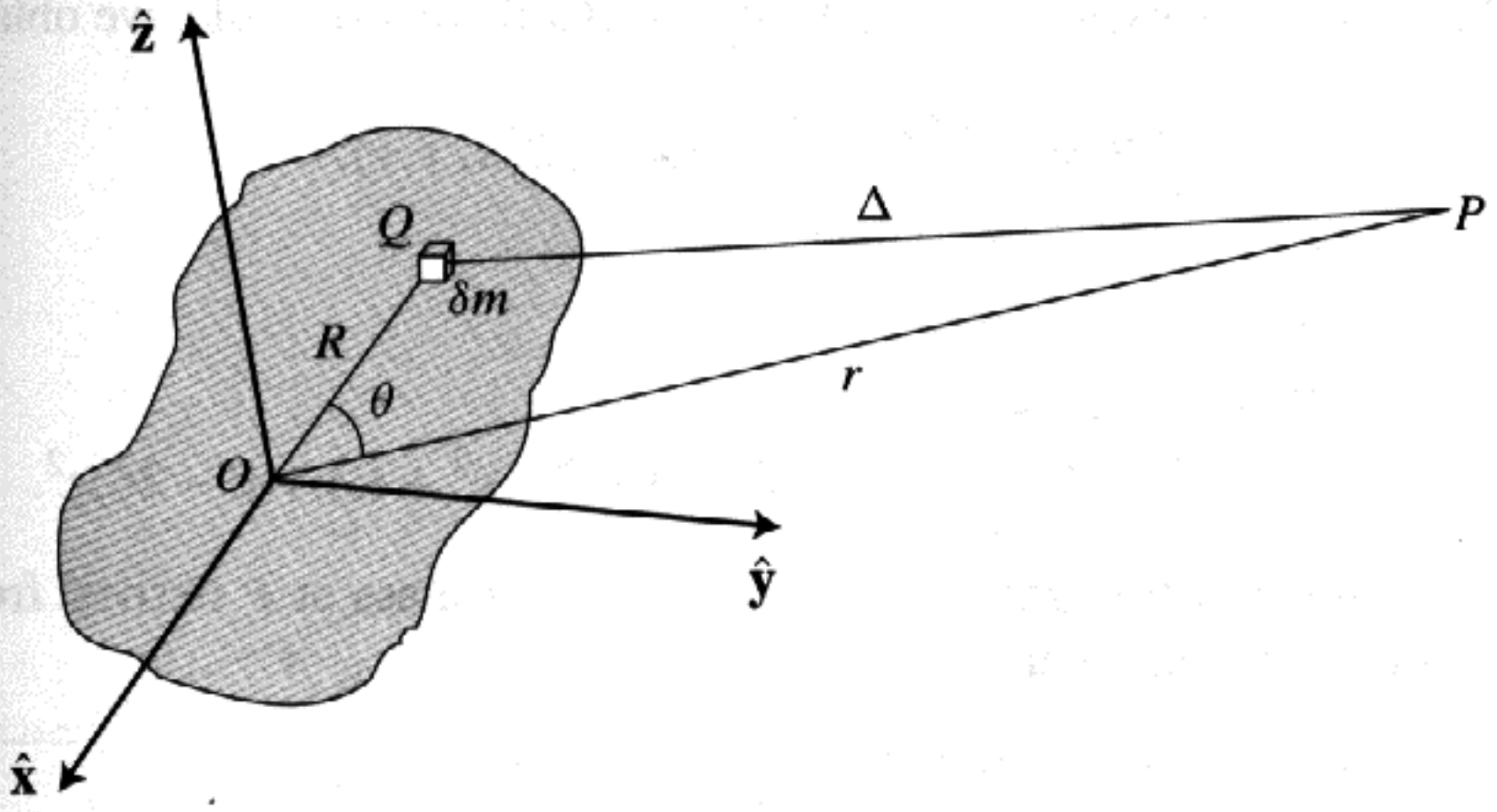

Fig. 5.5. A coordinate system with origin at the centre of mass O of a satellite with axes aligned with its principal moments of inertia. The point P is at a distance r from O. The small mass element δm at the point Q is at a distance R from O, and the line OQ makes an angle θ with the line OP.

where, as before, $m_s = \sum \delta m$ is the mass of the satellite. Because O is at the centre of mass of the satellite,

$$\sum \delta m \, R \cos\theta = 0. \tag{5.33}$$

We also have

$$\begin{aligned} 2\sum \delta m R^2 &= 2\sum \delta m(x^2 + y^2 + z^2) \\ &= \sum \delta m(y^2 + z^2) + \sum \delta m(z^2 + x^2) + \sum \delta m(x^2 + y^2) \\ &= \mathcal{A} + \mathcal{B} + \mathcal{C}. \end{aligned} \tag{5.34}$$

If we denote the moment of inertia of the body about the line OP by I, then

$$I = \sum \delta m \, R^2 \sin^2\theta \tag{5.35}$$

and, to the extent that (5.32) is a good approximation,

$$V = -\frac{\mathcal{G}m_s}{r} - \frac{\mathcal{G}(\mathcal{A} + \mathcal{B} + \mathcal{C} - 3I)}{2r^3}. \tag{5.36}$$

This is MacCullagh's formula (MacCullagh 1844a,b; Haughton 1855).

If we now let x, y, and z denote the coordinates of the point P, then x/r, y/r, and z/r are the direction cosines of P with respect to the principal axes of inertia and, from Eq. (5.27), we have

$$I = (\mathcal{A}x^2 + \mathcal{B}y^2 + \mathcal{C}z^2)/r^2. \tag{5.37}$$

On substituting this expression for I into MacCullagh's formula, we obtain

$$V = -\frac{\mathcal{G}m_s}{r} - \frac{\mathcal{G}}{2r^5} f(\mathcal{A}, \mathcal{B}, \mathcal{C}, x, y, z), \tag{5.38}$$

where

$$f(\mathcal{A}, \mathcal{B}, \mathcal{C}, x, y, z) = (\mathcal{B} + \mathcal{C} - 2\mathcal{A})x^2 + (\mathcal{C} + \mathcal{A} - 2\mathcal{B})y^2 + (\mathcal{A} + \mathcal{B} - 2\mathcal{C})z^2. \tag{5.39}$$

The components of the gravitational force per unit mass at P derived from the gradient of this potential are

$$F_x = -\frac{\partial V}{\partial x} = -\frac{\mathcal{G}m_s x}{r^3} + \frac{\mathcal{G}(\mathcal{B} + \mathcal{C} - 2\mathcal{A})x}{r^5} - \frac{5\mathcal{G}x}{2r^7} f(\mathcal{A}, \mathcal{B}, \mathcal{C}, x, y, z), \tag{5.40}$$

$$F_y = -\frac{\partial V}{\partial y} = -\frac{\mathcal{G}m_s y}{r^3} + \frac{\mathcal{G}(\mathcal{C} + \mathcal{A} - 2\mathcal{B})y}{r^5} - \frac{5\mathcal{G}y}{2r^7} f(\mathcal{A}, \mathcal{B}, \mathcal{C}, x, y, z), \tag{5.41}$$

$$F_z = -\frac{\partial V}{\partial z} = -\frac{\mathcal{G}m_s z}{r^3} + \frac{\mathcal{G}(\mathcal{A} + \mathcal{B} - 2\mathcal{C})z}{r^5} - \frac{5\mathcal{G}z}{2r^7} f(\mathcal{A}, \mathcal{B}, \mathcal{C}, x, y, z). \tag{5.42}$$

These forces exert a couple on a unit mass at P and an equal and opposite couple acts on the deformed body about its centre of mass. The latter couple has components

$$N_x = zF_y - yF_z = +3\mathcal{G}(\mathcal{C} - \mathcal{B})yz/r^5, \tag{5.43}$$

$$N_y = xF_z - zF_x = +3\mathcal{G}(\mathcal{A} - \mathcal{C})zx/r^5, \tag{5.44}$$

$$N_z = yF_x - xF_y = +3\mathcal{G}(\mathcal{B} - \mathcal{A})xy/r^5. \tag{5.45}$$

Euler's full equations of motion are

$$\mathcal{A}\dot{\omega}_x - (\mathcal{B} - \mathcal{C})\omega_y\omega_z = N_x, \tag{5.46}$$

$$\mathcal{B}\dot{\omega}_y - (\mathcal{C} - \mathcal{A})\omega_z\omega_x = N_y, \tag{5.47}$$

$$\mathcal{C}\dot{\omega}_z - (\mathcal{A} - \mathcal{B})\omega_x\omega_y = N_z, \tag{5.48}$$

where ω_x, ω_y, and ω_z are the projections of the spin vector on the principal axes. In our problem, we wish to calculate the rotational motion of a satellite due to the torque exerted on its quadrupole moment by a distant planet. We will assume that the spin axis of the satellite is normal to its orbital plane and that ω_x and ω_y are zero. We now denote the direction cosines of the planet with respect to the x axis and y axis by $x/r = \cos\psi$ and $y/r = \sin\psi$, respectively (see Fig. 5.6). In this case, Euler's equations of motion reduce to Eq. (5.48), which can be written

$$\mathcal{C}\ddot{\theta} - \frac{3}{2}(\mathcal{B} - \mathcal{A})\frac{\mathcal{G}m_p}{r^3}\sin 2\psi = 0, \tag{5.49}$$

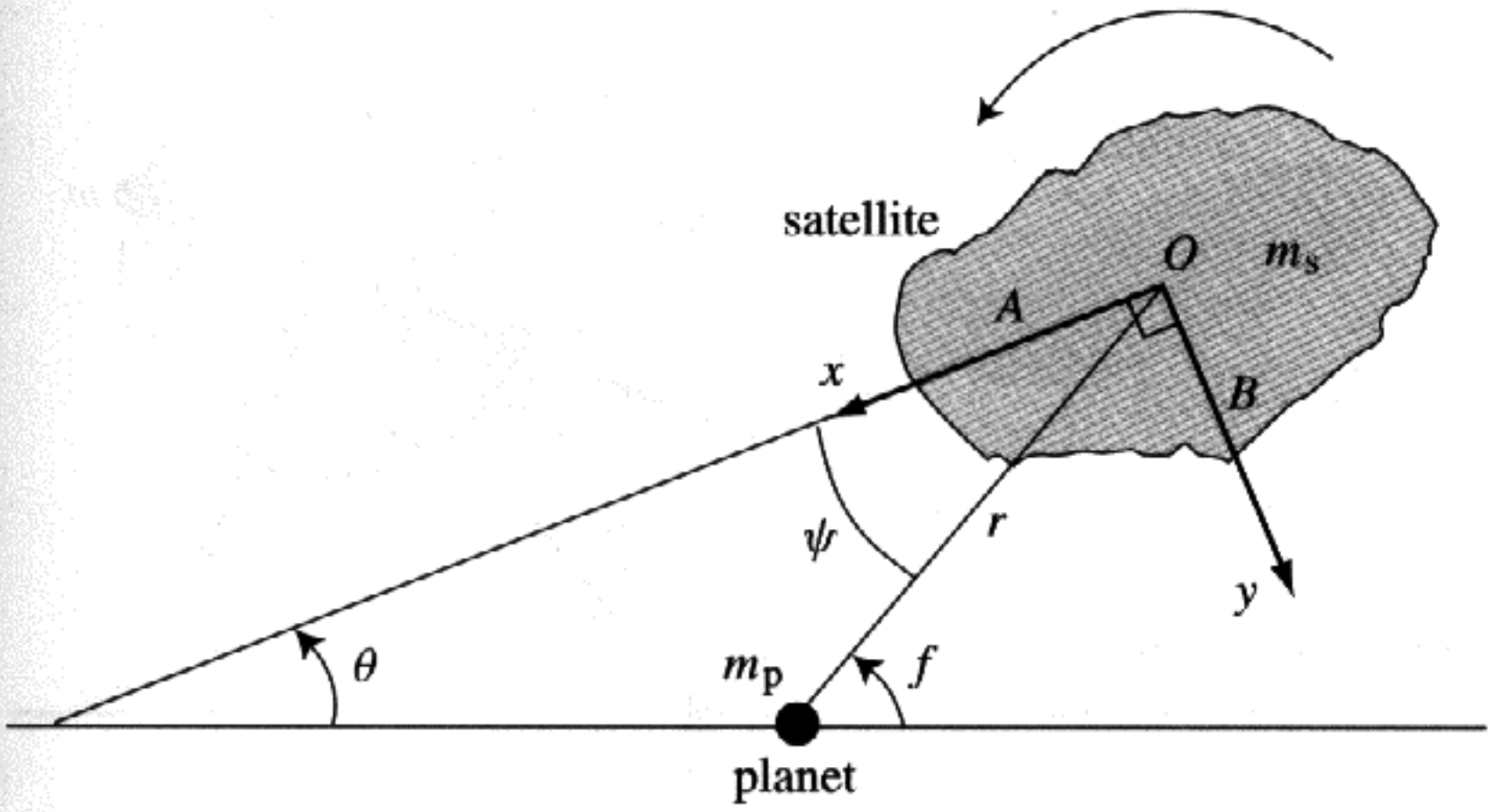

Fig. 5.6. Rotation of a satellite with its spin axis normal to the orbit plane. ψ is the angle between the planet–satellite line and the principal axis A associated with the minimum moment of inertia of the satellite. The angle θ is measured with respect to a direction fixed in inertial space.

where the angle θ is measured with respect to a direction fixed in inertial space. Note that, in some other formulations of the above equation of motion, for example, that given by Danby (1988), the sign of $\ddot{\theta}$ is negative rather than positive. This arises because Danby's choice of coordinate system implies that $\omega_z = -\dot{\theta}$.

We can obtain a simple, heuristic verification of Eq. (5.49) by considering the following. Represent a satellite with a permanent quadrupole moment by a spherical satellite with two equal, diametrically opposed point masses, m, embedded in its equatorial (and orbital) plane (see Fig. 5.7). Let the respective distances of these small masses from the planet be r_1 and r_2 and let r denote the distance between the centre of the satellite and the centre of the planet. The line joining the planet and satellite centres makes an angle ψ with the principal axis associated with $\mathcal{A}$, the minimum moment of inertia, that is, the line joining the two small masses, m.

If the satellite has a mean radius R_s, then the torque on the satellite due to the gravitational forces between the planet and the two small masses is $N_1 + N_2$, where

$$N_1 = +\mathcal{G}\frac{m_s m_p}{r_1^2} R_s \sin\alpha, \qquad N_2 = -\mathcal{G}\frac{m_s m_p}{r_2^2} R_s \sin\beta. \tag{5.50}$$

The angles α and β are defined in Fig. 5.7; the sign of N_1 is positive because it acts to increase θ. Applying the cosine and sine rules, we have

$$\sin\alpha = \frac{r}{r_1}\sin\psi, \qquad \sin\beta = \frac{r}{r_2}\sin\psi, \tag{5.51}$$

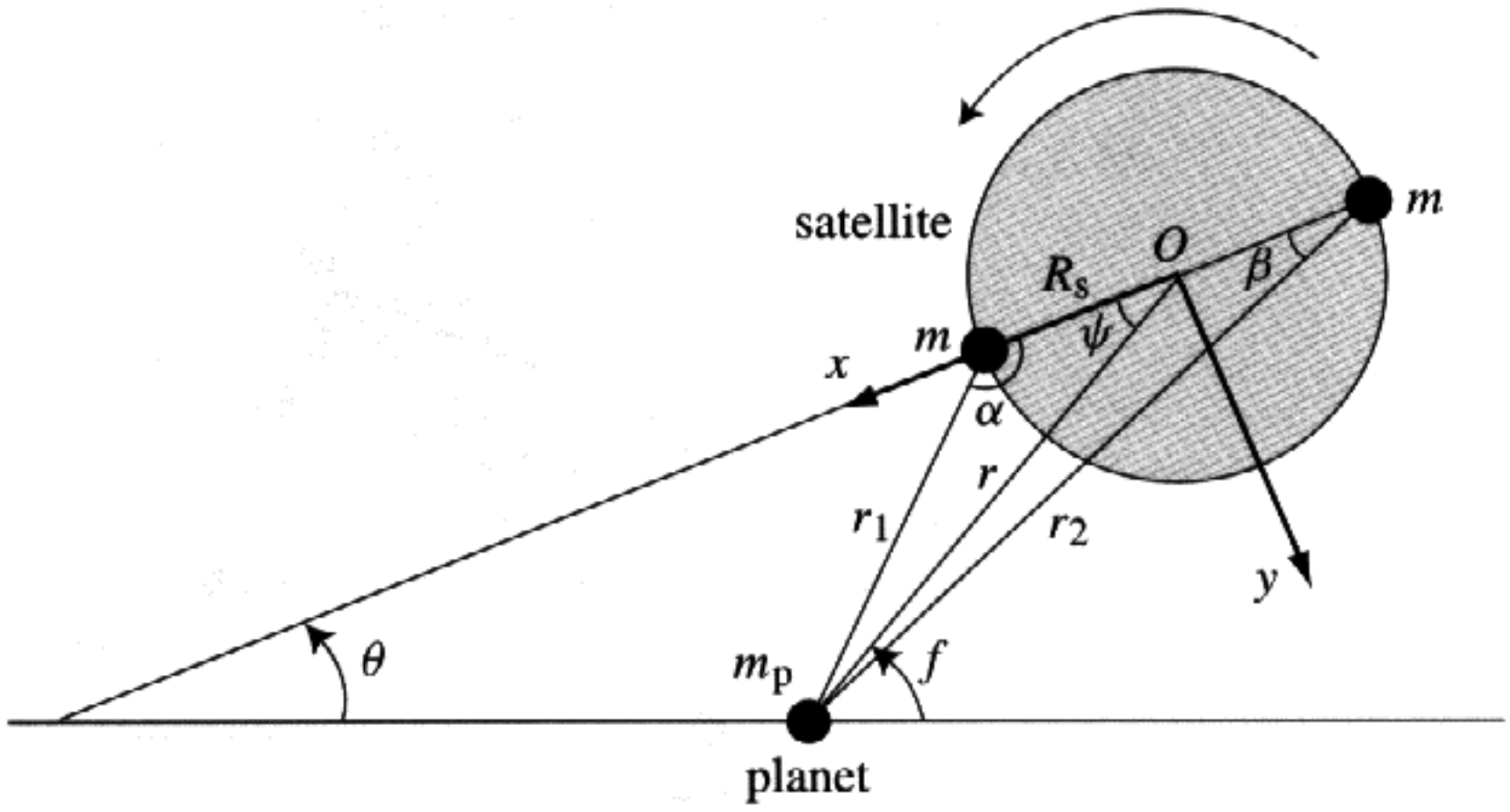

Fig. 5.7. Representation of a satellite with a quadrupole moment as a spherical object with two diametrically opposed small masses. The diameter joining the two masses defines the axis with the minimum moment of inertia and makes an angle ψ with the planet–satellite line (cf. Fig. 5.6).

and

$$\frac{1}{r_1^3} \approx \frac{1}{r^3}\left[1 - \frac{3}{2}\left(\frac{R_s}{r}\right)^2 + 3\frac{R_s}{r}\cos\psi\right], \tag{5.52}$$

$$\frac{1}{r_2^3} \approx \frac{1}{r^3}\left[1 - \frac{3}{2}\left(\frac{R_s}{r}\right)^2 - 3\frac{R_s}{r}\cos\psi\right]. \tag{5.53}$$

Hence the equation of motion for θ reduces to

$$C\ddot{\theta} - \frac{3}{2}\left(2mR_s^2\right)\frac{\mathcal{G}m_p}{r^3}\sin 2\psi = 0 \tag{5.54}$$

and, given that $\mathcal{B} - \mathcal{A} = 2mR_s^2$, the parallel with Eq. (5.49) is complete.

5.4 Spin–Orbit Resonance

The gravitational interaction between the orbital motion of a planet and the quadrupole moment of an attendant satellite results in small, short-period oscillations in the rotation rate of the satellite that, usually, are of little consequence. However, there are circumstances in which this is not the case. These arise when there is a simple integer, or near-integer, relationship between the spin period of a satellite and its orbital period, in which case there may be significant spin–orbit coupling. The following discussion is based on the pioneering work of Goldreich & Peale (1966, 1968), Wisdom, Peale & Mignard (1984), and Wisdom (1987a,b).

Consider the motion of a small satellite whose spin axis is normal to the plane of its fixed elliptical orbit. Let the long axis of the satellite make an angle θ with

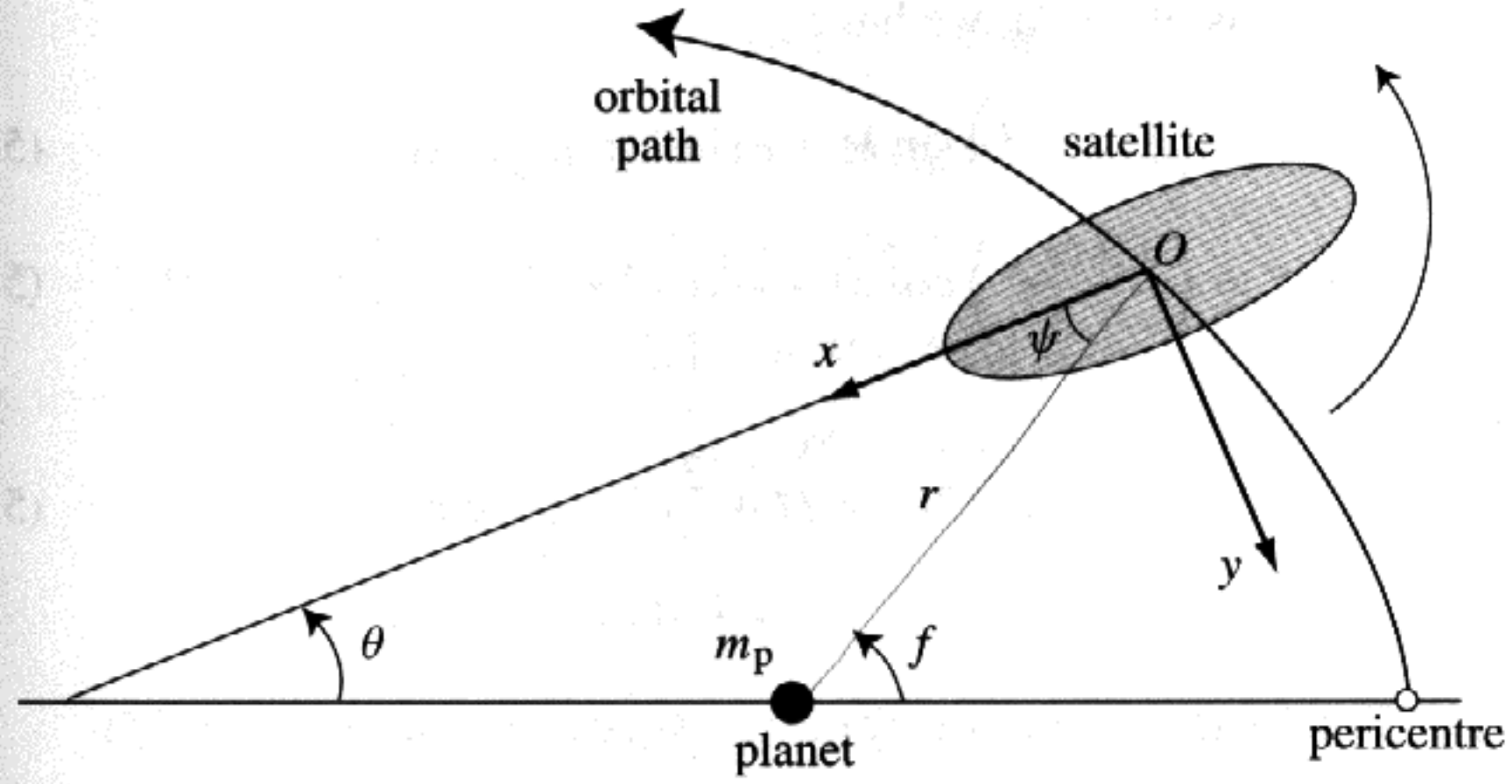

Fig. 5.8. The long axis of the satellite makes an angle θ with a reference axis that is fixed in inertial space, which we take to be the major axis of the satellite's fixed orbit.

a reference axis that is fixed in inertial space, which in this two-body, keplerian system we can take to be the major axis of the satellite's orbit. The long axis of the satellite makes an angle ψ with the satellite–planet centre line. Hence

$$\psi = f - \theta, \tag{5.55}$$

where f is the true anomaly (see Fig. 5.8). In the absence of tidal torques, the equation of motion for θ is (see Eq. (5.49))

$$C\ddot{\theta} - \frac{3}{2}(B - A)\frac{Gm_p}{r^3}\sin 2\psi = 0. \tag{5.56}$$

Because r and ψ vary with f, which is a nonlinear function of time, this equation is nonintegrable. However, in those cases of interest here, in which the spin rate $\dot{\theta}$ is commensurate with the mean motion n, we can derive an equation of motion that, although an approximation, is both useful and integrable.

Because we are interested in those cases for which $\dot{\theta}$ is a rational multiple of the mean motion, we introduce a new variable

$$\gamma = \theta - pM, \tag{5.57}$$

where p is a rational and M is the mean anomaly. Given that n is a constant, $\ddot{\theta} = \ddot{\gamma}$ and the equation of motion for γ is (cf. Eq. (5.56))

$$\ddot{\gamma} + \frac{3}{2}n^2\left(\frac{B - A}{C}\right)\left(\frac{a}{r}\right)^3 \sin(2\gamma + 2pM - 2f) = 0. \tag{5.58}$$

This equation can be expanded in a Fourier-like Poisson series in terms of e and M using standard expressions for $(a/r)^3$, $\sin f$, and $\cos f$ (see Sect. 2.5).

Including all terms of $\mathcal{O}(e^2)$, we have

$$\sin f = \left(1 - \frac{7}{8}e^2\right)\sin M + e\sin 2M + \frac{9}{8}e^2 \sin 3M, \tag{5.59}$$

$$\cos f = \left(1 - \frac{9}{8}e^2\right)\cos M + e(\cos 2M - 1) + \frac{9}{8}e^2 \cos 3M, \tag{5.60}$$

and

$$\left(\frac{a}{r}\right)^3 = 1 + 3e\cos M + \frac{3}{2}e^2(1 + 3\cos 2M). \tag{5.61}$$

We can write

$$\begin{aligned}\sin(2\gamma + 2pM - 2f) = {} & \sin 2\gamma(\cos 2pM \cos 2f + \sin 2pM \sin 2f) \\ & + \cos 2\gamma(\sin 2pM \cos 2f - \cos 2pM \sin 2f).\end{aligned} \tag{5.62}$$

Hence

$$\left(\frac{a}{r}\right)^3 \sin(2\gamma + 2pM - 2f) = [S_1 + S_2]\sin 2\gamma + [S_3 - S_4]\cos 2\gamma, \tag{5.63}$$

where

$$\begin{aligned} S_1 &= \left(\frac{a}{r}\right)^3 \cos 2pM \cos 2f, \qquad S_2 = \left(\frac{a}{r}\right)^3 \sin 2pM \sin 2f, \\ S_3 &= \left(\frac{a}{r}\right)^3 \sin 2pM \cos 2f, \qquad S_4 = \left(\frac{a}{r}\right)^3 \cos 2pM \sin 2f. \end{aligned} \tag{5.64}$$

To $\mathcal{O}(e^2)$, the S_i are given by

$$\begin{aligned} S_1 = {} & \frac{1}{2}[\cos 2(1-p)M + \cos 2(1+p)M] \\ & + \frac{1}{4}e[7\cos(3+2p)M + 7\cos(3-2p)M \\ & \quad - \cos(1+2p)M - \cos(1-2p)M] \\ & + \frac{1}{4}e^2[-5\cos 2(1+p)M - 5\cos 2(1-p)M \\ & \quad + 17\cos 2(2+p)M + 17\cos 2(2-p)M], \end{aligned} \tag{5.65}$$

$$\begin{aligned} S_2 = {} & \frac{1}{2}[\cos 2(1-p)M - \cos 2(1+p)M] \\ & + \frac{1}{4}e[-7\cos(3+2p)M + 7\cos(3-2p)M \\ & \quad - \cos(1-2p)M + \cos(1+2p)M] \\ & + \frac{1}{4}e^2[5\cos 2(1+p)M - 5\cos 2(1-p)M \\ & \quad - 17\cos 2(2+p)M + 17\cos 2(2-p)M], \end{aligned} \tag{5.66}$$

$$S_3 = \frac{1}{2}[\sin 2(1+p)M - \sin 2(1-p)M] + \frac{1}{4}e[7\sin(3+2p)M - 7\sin(3-2p)M + \sin(1-2p)M - \sin(1+2p)M] + \frac{1}{4}e^2[-5\sin 2(1+p)M + 5\sin 2(1-p)M + 17\sin 2(2+p)M - 17\sin 2(2-p)M], \tag{5.67}$$

$$S_4 = \frac{1}{2}[\sin 2(1+p)M + \sin 2(1-p)M] + \frac{1}{4}e[7\sin(3+2p)M + 7\sin(3-2p)M - \sin(1-2p)M - \sin(1+2p)M] + \frac{1}{4}e^2[-5\sin 2(1+p)M - 5\sin 2(1-p)M + 17\sin 2(2+p)M + 17\sin 2(2-p)M]. \tag{5.68}$$

Therefore, the equation of motion for γ, Eq. (5.58), can be written as

$$\ddot{\gamma} + \frac{3}{2}\frac{(\mathcal{B}-\mathcal{A})}{\mathcal{C}}n^2\left([S_1+S_2]\sin 2\gamma + [S_3-S_4]\cos 2\gamma\right) = 0. \tag{5.69}$$

Note that S_1 and S_2 only contain cosines, whereas S_3 and S_4 only contain sines. The equation is exact, but the S_i are infinite series in e and M and thus the equation is still nonintegrable. To progress, we must resort to approximations.

If the spin rate of the satellite is close to a spin–orbit resonance, then $\dot{\theta} \approx pn$ and γ is slowly varying, that is, $\dot{\gamma} \ll n$ and we can produce an approximate equation of motion by averaging all the terms in Eq. (5.69) over one orbital period while holding γ fixed. We then obtain

$$\ddot{\gamma} + \frac{3}{2}\frac{(\mathcal{B}-\mathcal{A})}{\mathcal{C}}n^2\left([\langle S_1\rangle + \langle S_2\rangle]\sin 2\gamma + [\langle S_3\rangle - \langle S_4\rangle]\cos 2\gamma\right) = 0, \tag{5.70}$$

where

$$\langle S_i\rangle = \frac{1}{2\pi}\int_0^{2\pi} S_i\,\mathrm{d}M, \qquad i = 1,2,3,4 \tag{5.71}$$

and it is now understood that γ refers to the averaged value. The S_i have to be evaluated for a particular value of the rational p corresponding to the particular spin–orbit resonance under consideration. Because cosines and sines with arguments that are integer multiples of M average out to zero over one orbital period, the only terms in S_i that make a nonzero contribution to the equation of motion are those cosine terms with zero arguments. For example, in the synchronous case for which $p = 1$, only those cosine terms with arguments containing $p - 1$ as a factor contribute to the equation of motion. Inspection of Eqs. (5.81) to

(5.84) shows that in this case, to $\mathcal{O}(e^2)$, we have

$$\left([\langle S_1\rangle + \langle S_2\rangle]\sin 2\gamma + [\langle S_3\rangle - \langle S_4\rangle]\cos 2\gamma\right)_{p=1} = \left(1 - \frac{5}{2}e^2\right)\sin 2\gamma. \quad (5.72)$$

If we carry out the same procedure for other values of p, then inspection of the same equations (or the equivalent set that contains terms of higher order in e) shows that only values of p that are an integer multiple of $1/2$ can contribute to the averaged equation of motion. In those cases, we can write

$$\ddot{\gamma} + \frac{3}{2}n^2\frac{(\mathcal{B}-\mathcal{A})}{\mathcal{C}}H(p,e)\sin 2\gamma = 0, \quad (5.73)$$

where, for example, to $\mathcal{O}(e^4)$,

$$H(-1,e) = +\frac{1}{24}e^4, \quad (5.74)$$

$$H(-1/2,e) = +\frac{1}{48}e^3, \quad (5.75)$$

$$H(0,e) = 0, \quad (5.76)$$

$$H(+1/2,e) = -\frac{1}{2}e + \frac{1}{16}e^3, \quad (5.77)$$

$$H(+1,e) = +1 - \frac{5}{2}e^2 + \frac{13}{16}e^4, \quad (5.78)$$

$$H(+3/2,e) = +\frac{7}{2}e - \frac{123}{16}e^3, \quad (5.79)$$

$$H(+2,e) = +\frac{17}{2}e^2 - \frac{115}{6}e^4, \quad (5.80)$$

$$H(+5/2,e) = +\frac{845}{48}e^3, \quad (5.81)$$

$$H(+3,e) = +\frac{533}{16}e^4. \quad (5.82)$$

Inspection of the eccentricity function, $G_{lpq}(e)$, defined by Kaula (1966) shows that

$$H(p,e) = G_{20(2p-2)}(e) \quad (5.83)$$

and that, except for the case $p = 0$, $H(p,e) = \mathcal{O}\left(e^{2|p-1|}\right)$.

Thus, by introducing an approximation, we have reduced the full equation of motion, Eq. (5.56), to the pendulum equation, which we can write as

$$\ddot{\gamma} = -[\text{sign}\, H(p,e)]\frac{1}{2}\omega_0^2\sin 2\gamma, \quad (5.84)$$

where

$$\omega_0 = n\left[3\left(\frac{\mathcal{B}-\mathcal{A}}{\mathcal{C}}\right)|H(p,e)|\right]^{1/2} \quad (5.85)$$

is the libration frequency. In the presence of a tidal torque acting to brake the spin of the satellite, a term representing the mean tidal torque averaged over one orbital period, $\langle N_s \rangle$, can be added to the averaged equation of motion to give

$$\ddot{\gamma} = -[\text{sign}\, H(p,e)]\frac{1}{2}\omega_0^2 \sin 2\gamma + \langle N_s \rangle / C. \tag{5.86}$$

If

$$|\langle N_s \rangle| / C < \frac{1}{2}\omega_0^2 \tag{5.87}$$

then the sign of $\ddot{\gamma}$ must reverse periodically and thus it is possible for the satellite to be trapped in a spin–orbit resonance for which $\langle \dot{\theta} \rangle = pn$. If Eq. (5.87), the *strength criterion,* is satisfied, then the mean torque due to the resonant interaction between the planet and the quadrupole moment of the satellite compensates for the mean tidal torque acting to change the spin period of the satellite, $\langle \ddot{\gamma} \rangle = 0$, and γ librates about an equilibrium value γ_0 given by

$$\gamma_0 = \frac{1}{2}\sin^{-1}\left[\frac{2\langle N_s \rangle}{-[\text{sign}\, H(p,e)]\omega_0^2 C}\right]. \tag{5.88}$$

The equilibrium orientation of the satellite and the sign of γ_0 are determined by the sign of $H(p,e)$. For small displacements of γ from γ_0, the sign of $\ddot{\gamma}$ must be such as to return γ to the equilibrium displacement, γ_0. If the mean tidal torque is weak in comparison with the resonant torque, that is, if

$$|\langle N_s \rangle| / C \ll \frac{1}{2}\omega_0^2 \tag{5.89}$$

then, if $H(p,e) > 0$, $\gamma_0 \approx 0$ or π and the long axis of the satellite points towards the planet on passage of the satellite through pericentre. Conversely, if $H(p,e) < 0$, $\gamma_0 \approx \pi/2$ or $3\pi/2$ and the long axis of the satellite points in a direction perpendicular to the planet–satellite line on passage of the satellite through pericentre.

We now consider the rotation of Mercury and give a simple, physical interpretation of the averaged equation of motion. The case of Mercury is particularly interesting because it was only after radar observations revealed that the planet is trapped in a 3:2 spin–orbit resonance with the Sun, rather than the expected 1:1 synchronous state, that the dynamics of spin–orbit resonance was first investigated. A good history of these events has been given by Goldreich & Peale (1968). The rotational and orbital motions of Mercury in an inertial reference frame are shown in Fig. 5.9.

The spin period of the planet is 58.65 d, while its orbital period is $87.97 = 1.5 \times 58.65$ d. Thus, the planet rotates on its axis three times while it orbits the Sun twice and on successive passages of Mercury through perihelion, opposite faces of the planet are presented to the Sun. The physical meaning of the angle

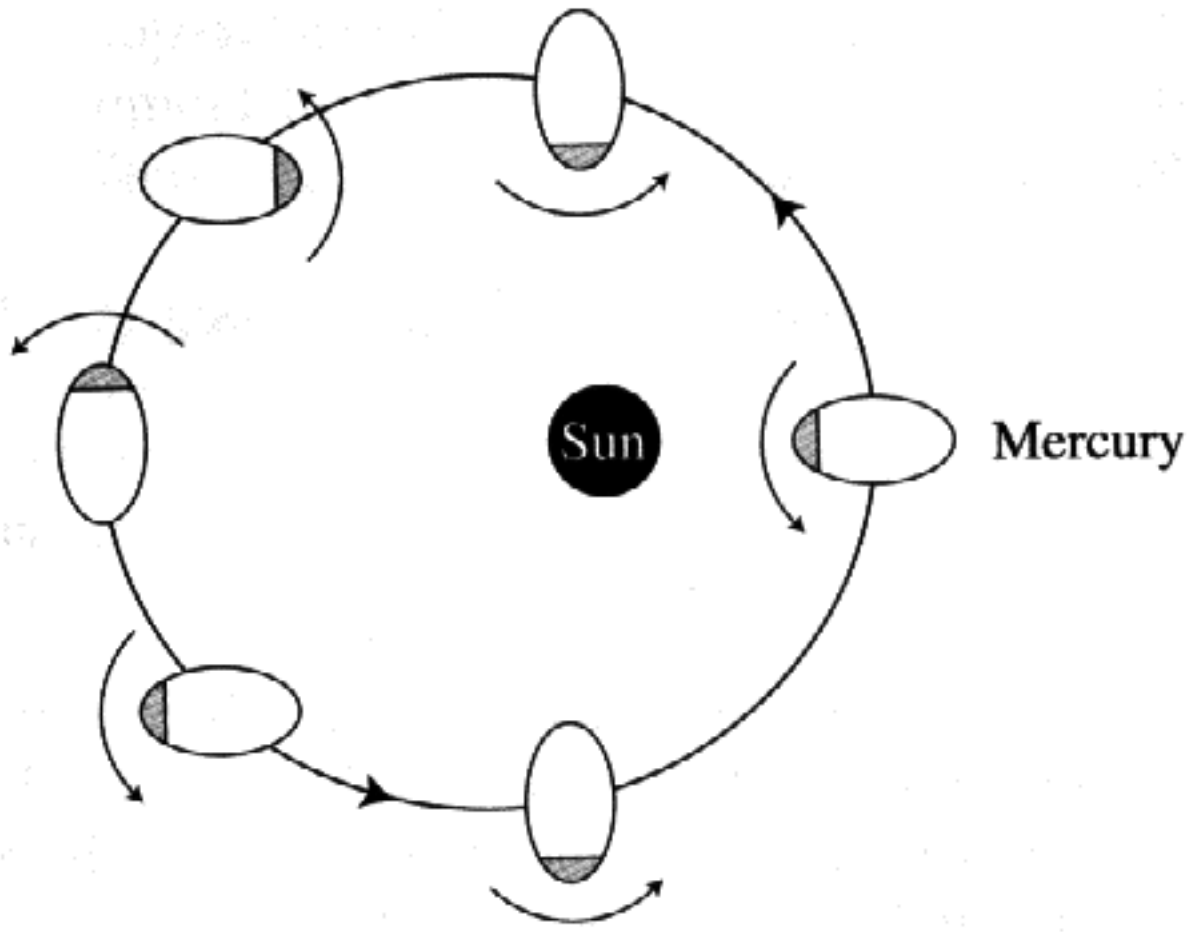

Fig. 5.9. In an inertial frame centred on the Sun, the planet Mercury completes 3/2 rotations each orbital period.

γ is that it describes the orientation of the long axis of the satellite on passage of the satellite through pericentre, that is, it is a *stroboscopic angle* that is evaluated when $M = 0$. Given that $H(p, e) \approx +(7/2)e > 0$, we expect that $\gamma \approx 0$ and that at perihelion the long axis of the planet points towards the Sun (Fig. 5.10). However, it is possible for γ to librate about the equilibrium value with an amplitude $\leq \pi/2$. If Mercury were trapped in the $p = +1/2$ resonance, for which $H(p, e) < 0$, then we would expect the orientation of the planet to be as shown in Fig. 5.11.

Figure 5.10a shows the motion of the Sun in a reference frame centred on Mercury and rotating with the planet's mean, resonant spin rate, $(3/2)n$, where n is Mercury's mean motion. The points on the looped path indicate the position of the Sun at equal intervals of time. The path of the Sun in this rotating frame is closed only because the spin–orbit resonance exists and it is this crucial fact that validates our use of the averaging method. The average gravitational interaction between the quadrupole moment of the planet and the Sun can be modelled by spreading the mass of the Sun along this closed path in such a way that the local line density is proportional to the time spent by the Sun in that part of the path. This line density is inversely proportional to the spacing of the points shown in Fig. 5.10a. The angle γ can now be interpreted as the deviation of the long axis of the planet from the planet–perihelion direction in the rotating frame (Fig. 5.10a). From the symmetry of this figure, we further deduce that the gravitational interaction could be modelled by replacing the mass distribution of the Sun with a circular distribution of uniform line density that does not contribute to the torque plus two point masses, $f m_{\text{sun}}$, positioned as shown in

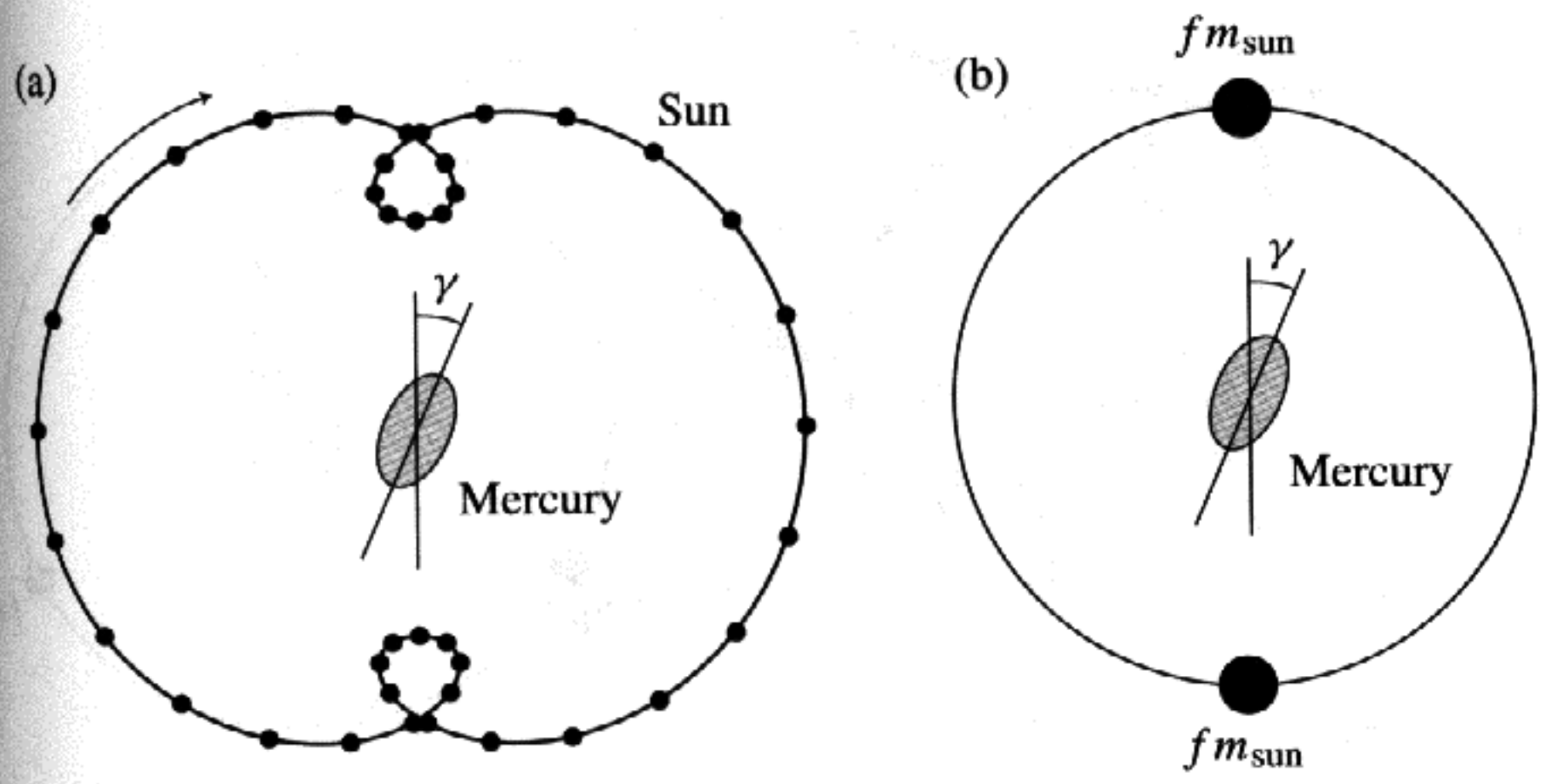

Fig. 5.10. (a) The motion of the Sun as seen in a reference frame centred on Mercury and rotating with Mercury's resonant spin rate, $(3/2)n$, where n is Mercury's mean motion. The gravitational interaction between the quadrupole moment of Mercury and the Sun can be modelled by spreading the mass of the Sun around the closed path with a local line density proportional to the time spent in that part of the path (the points on the closed path show successive positions of the Sun at equal intervals of time) or by two point masses, fm_{sun} where $f = (1/2)H(3/2, e)$, placed as shown in (b).

Fig. 5.10b, where

$$f = \frac{1}{2}H(p, e) \approx \frac{7}{4}e \tag{5.90}$$

and m_{sun} is the mass of the Sun.

A closed path in a rotating reference frame, as shown in Fig. 5.11, is a necessary but not a sufficient condition for spin–orbit coupling. Equations (5.65) and

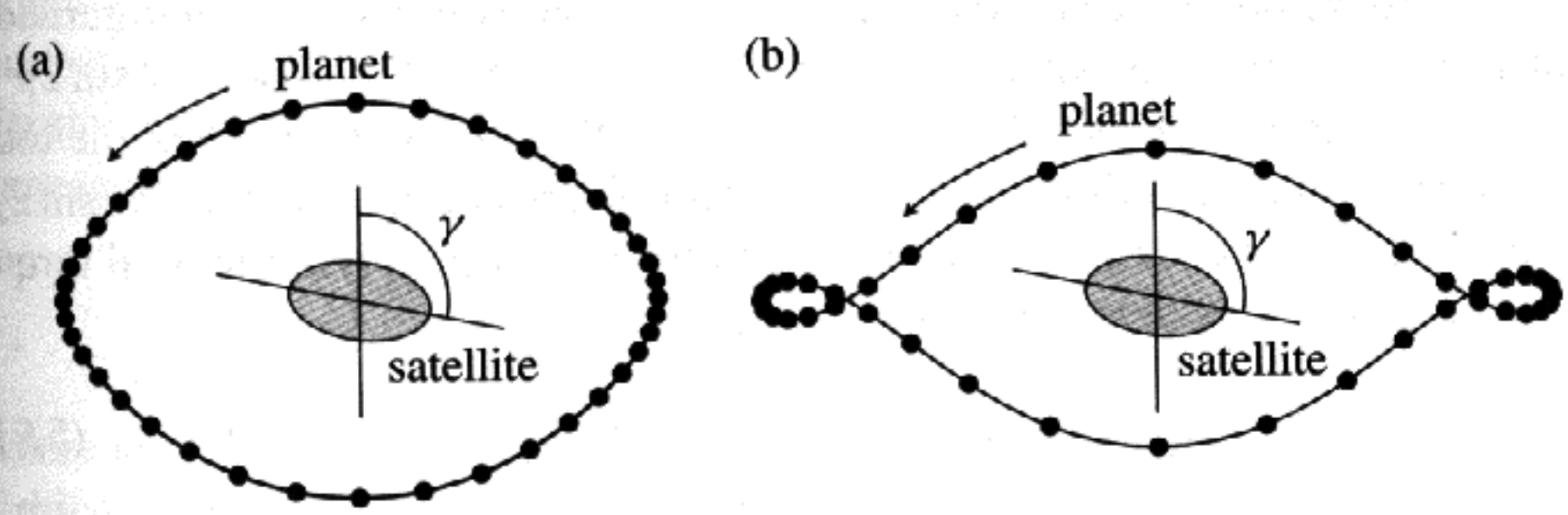

Fig. 5.11. The orientation of a satellite trapped in a $p = +1/2$ resonance is anomalous in that on passage of the satellite through pericentre its long axis points in a direction perpendicular to the planet–satellite line. The path of the planet in a rotating reference frame centred on the satellite is shown for (a) a small eccentricity and (b) a large eccentricity.

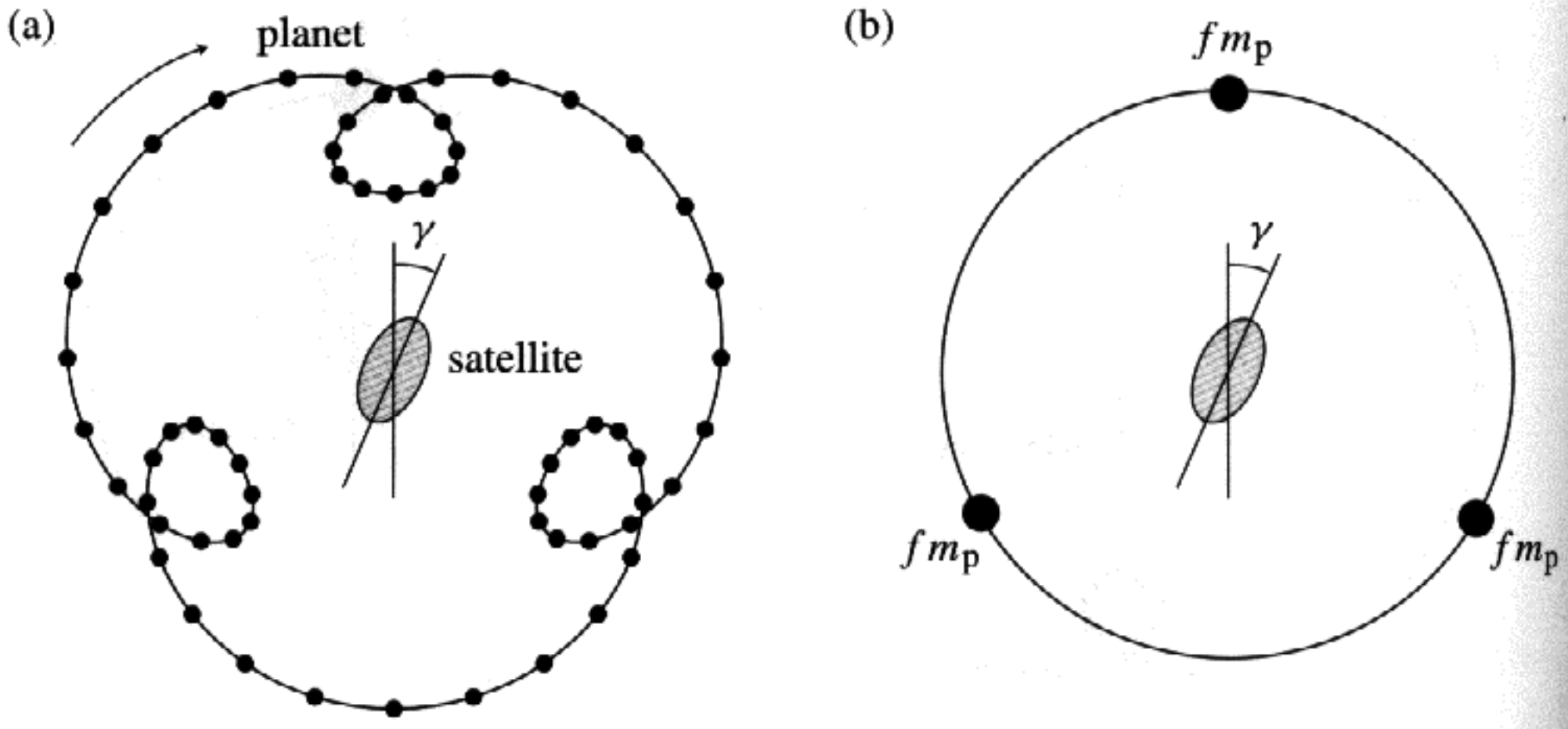

Fig. 5.12. (a) The path of a planet in a reference frame centred on a satellite and rotating with the satellite's mean spin rate, in this case $(4/3)n$, where n is the satellite's mean motion. The averaged gravitational torque on the planet due to the satellite's quadrupole moment can be modelled by replacing the looped path of the planet in the rotating reference frame by a circular distribution of mass plus three point masses placed as shown in (b).

(5.56) show that p must also be an integer multiple of $1/2$ (this is determined by the twofold symmetry of the satellite's gravitational potential). It is worth considering why other values of p do not contribute to any resonant interaction. In Fig. 5.12 we show the motion of a planet as seen in a reference frame centred on a satellite and rotating with the satellite's mean rotation rate, in this case $(4/3)n$, where n is the satellite's mean motion. From the shape of the closed path in Fig. 5.12a, we can see that in this case the average gravitational force of the planet could be modelled by replacing the looped path by a circular distribution of mass and three equal point masses (see Fig. 5.12b). Now compare the configuration shown in Fig. 5.10b with that shown in Fig. 5.12b. In Fig. 5.10b, if $N \sin 2\gamma$ is the torque acting on the satellite due to one of the point masses, then the total torque on the satellite acting to restore the equilibrium configuration is $2N \sin 2\gamma$. However, in the case depicted in Fig. 5.12b for which $p = 4/3$, the total torque acting to change γ is determined by

$$N \sin 2\gamma + N \sin 2\left(\frac{\pi}{3} + \gamma\right) - N \sin 2\left(\frac{\pi}{3} - \gamma\right) = 0 \tag{5.91}$$

and the system is neutrally stable.

The special case of $p = 0$ is shown in Fig. 5.13. The torque δN on the satellite due to the mass element δm is given by

$$\delta N = \frac{3}{2}(\mathcal{B} - \mathcal{A})\frac{\mathcal{G}\,\delta m}{r^3} \sin 2\psi. \tag{5.92}$$

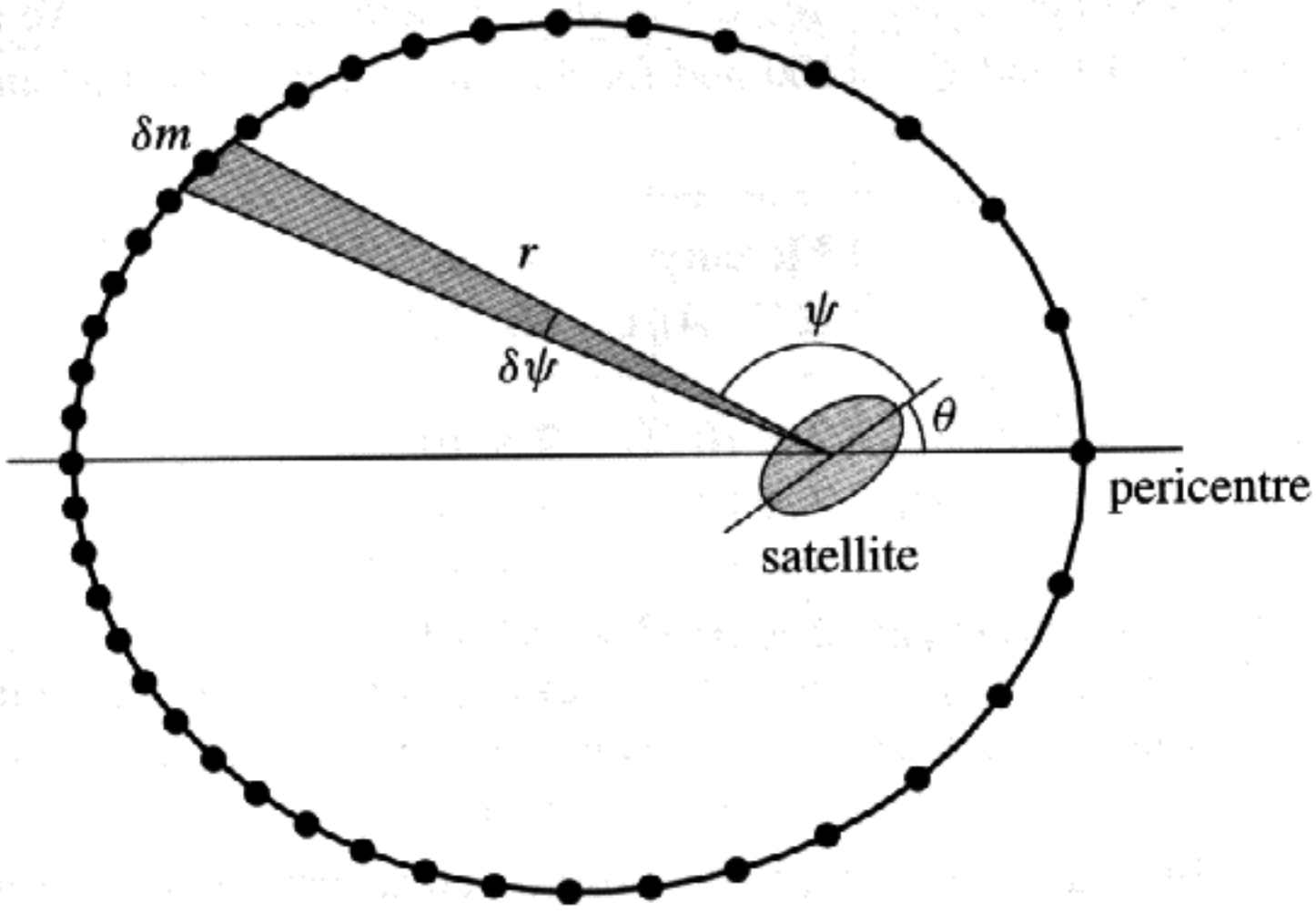

Fig. 5.13. The path of a planet in an inertial reference frame centred on the satellite. If $p = 0$, then the orientation of the satellite is fixed in inertial space and there is no resonant interaction with the planet.

From Kepler's law of areas, we obtain

$$\delta m = \frac{r^2 \delta\psi}{2\pi a^2 (1 - e^2)^{1/2}}. \tag{5.93}$$

Hence, the total torque on the satellite is given by

$$N = \frac{3(\mathcal{B} - \mathcal{A})\mathcal{G}}{4\pi a^3 (1 - e^2)^{3/2}} \int_0^{2\pi} [1 + e\cos(\psi + \theta)] \sin 2\psi \, \mathrm{d}\psi, \tag{5.94}$$

and given that the satellite is not rotating in inertial space, θ is fixed and the integral is zero.

For a satellite to be trapped in a particular spin–orbit resonance, the torque on the satellite due to the resonance must exceed that due to tidal drag. From the strength criterion, Eq. (5.79) and Eq. (5.2), we calculate that $(\mathcal{B} - \mathcal{A})/\mathcal{C}$ must exceed a critical value given by

$$\left(\frac{\mathcal{B} - \mathcal{A}}{\mathcal{C}}\right)_{\text{critical}} = \frac{5}{2}\frac{k_2}{Q}\left(\frac{R_\mathrm{s}}{a}\right)^3 \frac{m_\mathrm{p}}{m_\mathrm{s}} \frac{1}{|H(p, e)|}, \tag{5.95}$$

where m_p is the mass of the primary and we have assumed that $\mathcal{C} \approx (2/5) m_\mathrm{s} R_\mathrm{s}^2$. Critical values of $(\mathcal{B} - \mathcal{A})/\mathcal{C}$ for a series of spin–orbit resonances in the Sun–Mercury and the Earth–Moon systems are listed in Table 5.1. The orbital eccentricities of the Moon and Mercury are, respectively, 0.0549 and 0.206, while $(\mathcal{B} - \mathcal{A})/\mathcal{C} \approx 2.28 \times 10^{-4}$ for the Moon (Yoder 1995) and it is reasonable to assume that $(\mathcal{B} - \mathcal{A})/\mathcal{C}$ for Mercury is comparable. Inspection of Table 5.1 shows that there is certainly no problem in understanding the stability of Mercury's

Table 5.1. Critical values of $(\mathcal{B} - \mathcal{A})/\mathcal{C}$ for Mercury and the Moon. We assume for Mercury that $k_2 \approx 0.1$ and $Q = 100$ and for the Moon that $k_2 \approx 0.03$ and $Q = 27$ (Yoder 1995).

p	Mercury $(\mathcal{B} - \mathcal{A})/\mathcal{C}$	Moon $(\mathcal{B} - \mathcal{A})/\mathcal{C}$
+3	2×10^{-8}	7×10^{-5}
+5/2	7×10^{-9}	7×10^{-6}
+2	3×10^{-9}	8×10^{-7}
+3/2	2×10^{-9}	10^{-7}
+1	10^{-9}	2×10^{-8}

present spin–orbit state, or that of the Moon. However, if we allow that the spins of both of these bodies have been tidally braked and that their initial orbital periods were short, then we do need to understand not only how these bodies came to be trapped in their present spin–orbit states but also how they were able to evolve through many other strong resonances without trapping.

5.5 Capture into Resonance

That there is a problem with understanding capture into resonance can be seen by following the evolution of a satellite's spin rate on encounter with a spin–orbit resonance. We assume that, initially, $\dot{\theta} > pn$ and that tides act to brake the spin of the satellite. Thus, initially, $\dot{\gamma} > 0$ and the resonance is approached from above (Fig. 5.14). The equation of motion of the resonant argument, γ, in the presence of drag, is

$$\mathcal{C}\ddot{\gamma} + \frac{3}{2}(\mathcal{B} - \mathcal{A})n^2 H(p, e) \sin 2\gamma = \langle N_s \rangle. \tag{5.96}$$

Integrating with respect to time, we obtain the *energy integral*

$$\frac{1}{2}\mathcal{C}\dot{\gamma}^2 - \frac{3}{4}(\mathcal{B} - \mathcal{A})n^2 H(p, e) \cos 2\gamma = E, \tag{5.97}$$

where E, the total energy, is given by

$$E = \langle N_s \rangle \gamma + E_0 \tag{5.98}$$

and E_0 is a constant determined by the initial conditions. For the energy equation, Eq. (5.97), to have physical solutions ($\dot{\gamma}^2 > 0$), we must have

$$E \geq -\frac{3}{4}(\mathcal{B} - \mathcal{A})n^2 |H(p, e)|. \tag{5.99}$$

If $E > +(3/4)(\mathcal{B} - \mathcal{A})n^2|H(p, e)|$, then the sign of $\dot{\gamma}$ does not change and the motion of γ is one of *circulation*. However, given that $\langle N_s \rangle < 0$, tidal forces act to reduce E and resonance encounter occurs when $\dot{\gamma}$ is reduced to zero.

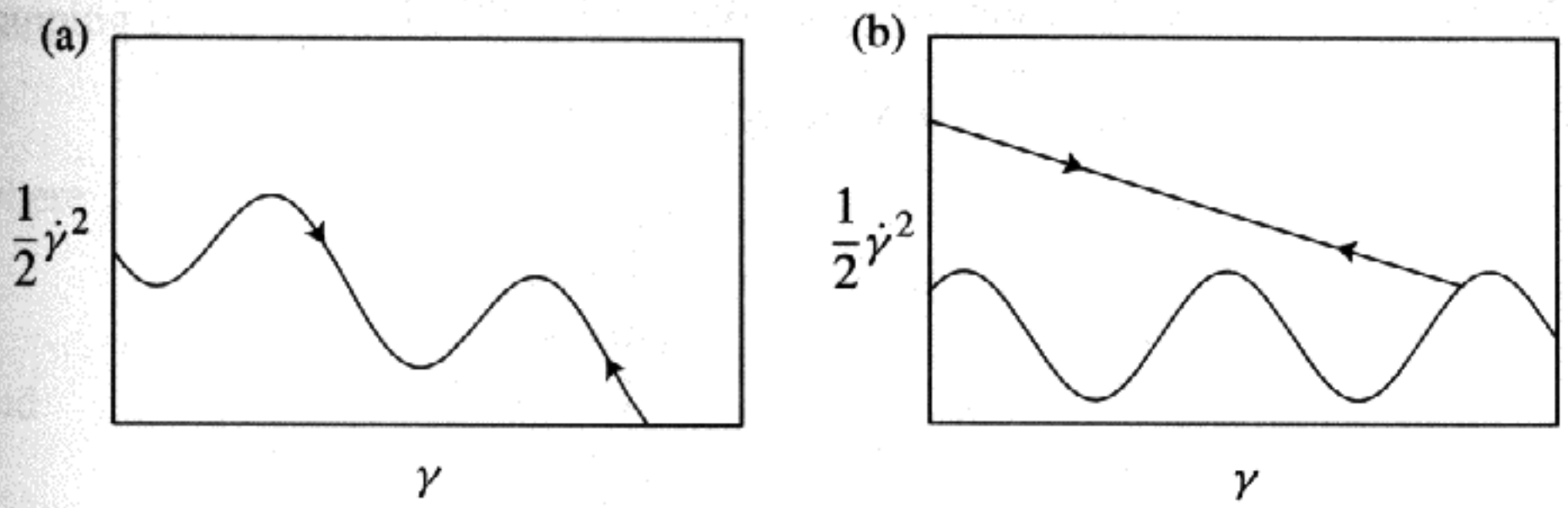

Fig. 5.14. (a) Variation of $(1/2)\dot{\gamma}^2$ with the resonant argument γ. (b) Separation of the variation of $(1/2)\dot{\gamma}^2$ with γ into a potential term that varies sinusoidally with γ and a term due to the tidal torque that decreases linearly with increasing γ. In the latter treatment, $(1/2)\dot{\gamma}^2$ is given by the *difference* of these two terms.

In Fig. 5.14a we show the total variation of $\dot{\gamma}^2$ with γ, while in Fig. 5.14b we separate the variation of $\dot{\gamma}^2$ into two components, one due to the potential term that varies sinusoidally with γ and a drag term that decreases linearly with increasing γ before resonance encounter and increases linearly with decreasing γ after resonance encounter. In the latter representation, the variation of $\dot{\gamma}^2$ with γ is given by the *difference* of the two terms. If $\langle N_s \rangle$ is constant, then the equation of motion is perfectly reversible: The sign of $\dot{\gamma}$ changes on resonance encounter, but the trajectory of the system in $(\gamma, \dot{\gamma})$ space after encounter duplicates that before encounter and capture into resonance cannot occur.

Goldreich & Peale (1968) explain this passage through resonance without capture using the following "pendulum" analogy. While the pendulum is circulating, a constant torque acts to brake its rotation. Thus, after a while, the pendulum will pass over its point of support for the last time (in the initial direction for which $\dot{\gamma} > 0$) and its rotation rate will be reduced to zero. The sense of rotation of the pendulum then reverses. However, both the magnitude and sign of the torque remain unchanged and thus the torque now acts to increase the rotation rate of the pendulum. Whatever energy was removed from the pendulum before it was braked is now resupplied and the pendulum swings back over its point of support and the magnitude of the rate of rotation (with $\dot{\gamma} < 0$) then continues to increase.

Given that the amplitude of the sinusoidal potential term in the energy equation is constant, it follows that for capture into resonance to occur, (a) $\langle N_s \rangle$ must somehow vary with $\dot{\gamma}$ and (b) during the last swing of the pendulum, during which the sign of $\dot{\gamma}$ reverses, the decrease in E before resonance encounter ($\dot{\gamma} = 0$) must be greater than the increase in E after resonance encounter, preventing the pendulum from swinging back over its point of support.

As we have already noted, the incorporation of energy dissipation into tidal theory is in many ways poorly developed. However, Goldreich & Peale (1966,

Table 5.2. Physical and orbital quantities for Mercury and the Moon.

Quantity	Mercury	Moon
k_2	0.1	0.03
Q	100	27
e	0.206	0.0549
$(\mathcal{B}-\mathcal{A})/\mathcal{C}$	10^{-4}	2.28×10^{-4}
$H(p,e)$	0.65	0.99
$T_{\text{libration}}$	17 y	2.88 y
γ_0	2 arcsec	9.6 arcsec
$2\pi/\dot{\theta}_{\text{initial}}$	9 h	9 h
T_{despin}	5×10^9 y	3×10^7 y
$\langle N_{\text{s}}\rangle\pi/U$	10^{-4}	6×10^{-4}

1968) give several plausible models of tidal dissipation that allow $\langle N_{\text{s}}\rangle$ to vary with $\dot{\gamma}$ and they have used these models to estimate the probability of capture into resonance. We will describe two of these models, both based on that due to Darwin (1908), but before doing so we need to estimate the magnitudes of the various terms in the energy equation. Tidal forces in the solar system are extremely weak and produce significant changes in some spin rates and orbital periods only because they act over billions of years. Using the values of k_2 and Q, etc., listed in Table 5.2, we calculate that if the initial spin periods $(2\pi/\dot{\theta}_{\text{initial}})$ of Mercury and the Moon were, say, 9 hours, then the times needed to brake these bodies were 5×10^9 and 3×10^7 years, respectively, implying that the Mercury–Sun spin–orbit resonance may be comparatively young. The lag angles, γ_0, given by Eq. (5.88) are only a few arcseconds and if we denote the amplitude of the potential term, $(3/4)(\mathcal{B}-\mathcal{A})n^2H(p,e)\cos2\gamma$, in the energy equation by U, then $\langle N_{\text{s}}\rangle\pi/U \ll 1$. We also note that the libration periods, $T_{\text{libration}} = 2\pi/\omega_0$ (using Eq. (5.85)), are greater than the orbital periods, but not by large factors.

Using Darwin's procedure for calculating the tidal torque on a satellite due to the tide raised on it by a planet, we expand the tidal potential in a Fourier time series and assume that each component raises an equilibrium tide on the satellite. The effects of tidal dissipation are then modelled by giving each component a phase shift such that the component either leads or lags the associated term in the potential. In our first model, we assume that the magnitudes, but not the signs, of the phase shifts are independent of the tidal frequencies. In this case, the mean tidal torque is given by

$$\langle N_{\text{s}}\rangle = -D\sum_{h=-\infty}^{\infty}[H(h,e)]^2\ \text{sign}\,(\dot{\theta}-hn), \tag{5.100}$$

where h is a half-integer, D is a positive constant given by Eq. (5.3), and we have assumed that the spin axis of the satellite is normal to its orbital plane. For

trapping in the pth resonance, $\dot{\theta} - pn = \dot{\gamma}$ and we can write

$$\langle N_s \rangle = -W - Z \operatorname{sign}(\dot{\gamma}), \tag{5.101}$$

where

$$W = +D \sum_{h \neq p} [H(h, e)]^2 \operatorname{sign}(p - h) \tag{5.102}$$

and

$$Z = +D [H(p, e)]^2 . \tag{5.103}$$

The rate of change of energy is given by

$$\frac{dE}{dt} = \langle N_s \rangle \dot{\gamma} . \tag{5.104}$$

Hence, the energy changes with γ according to

$$\int dE = \int_{\gamma_1}^{\gamma_2} \langle N_s \rangle \, d\gamma . \tag{5.105}$$

Because $\pi \langle N_s \rangle \ll (3/4)(\mathcal{B} - \mathcal{A}) n^2 H(p, e)$, the slopes of the straight lines in Fig. 5.15 are negligible and we can assume that in all integrations $\gamma_2 - \gamma_1 = \pi$.

Because the initial conditions are unspecified, the energy at the point P, where $\dot{\gamma}$ is first reduced to zero (Fig. 5.15), can lie anywhere in the range E_0' to $E_0' + \Delta E$, where

$$\Delta E = (W + Z)\pi . \tag{5.106}$$

On encounter with the pth resonance the sign of the $h = p$ term in Eq. (5.101) changes. Before resonance encounter, $\dot{\gamma} > 0$ and

$$\langle N_s \rangle = -W - Z, \tag{5.107}$$

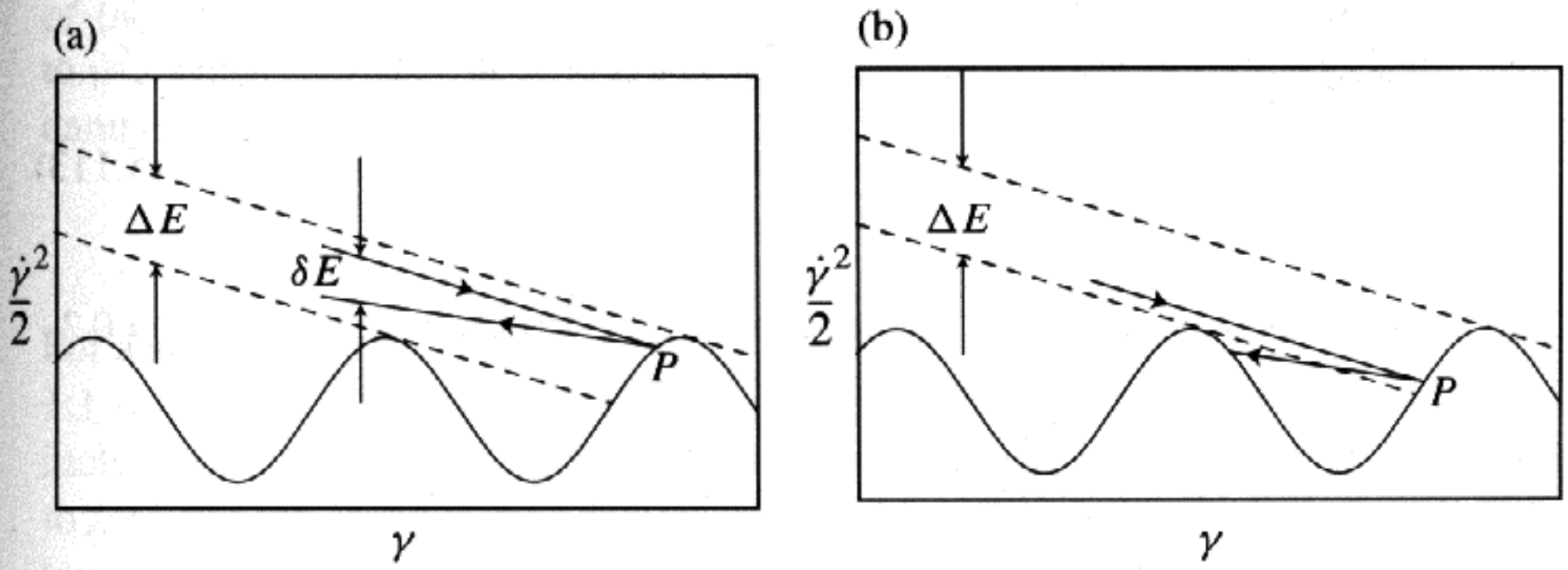

Fig. 5.15. Capture into resonance depends on the magnitude and sign of δE and the value of γ at the location P where $(1/2)\dot{\gamma}^2$ is first reduced to zero. The locations of P show an encounter with a resonance (a) without capture and (b) with capture. The capture probability is given by $|\delta E / \Delta E|$ and capture is certain if $\delta E < 0$ and $|\delta E| > |\Delta E|$.

and after resonance encounter, $\dot{\gamma} < 0$ and

$$\langle N_s \rangle = -W + Z. \tag{5.108}$$

Thus, on resonance encounter, the magnitude of $\langle N_s \rangle$ decreases by $2Z$. It follows that the decrease in E over one libration period is given by

$$\delta E = 2Z\pi \tag{5.109}$$

and that the probability P_p of capture into the pth resonance is given by

$$P_p = \frac{2Z}{Z+W} = \frac{2[H(p,e)]^2}{[H(p,e)]^2 + \sum_{h \neq p} [H(p,e)]^2 \operatorname{sign}(p-h)}. \tag{5.110}$$

In this case, the probability of capture does not depend on either $(\mathcal{B}-\mathcal{A})/\mathcal{C}$ or (assuming that the strength criterion, Eq. (5.87), is satisfied) on the magnitude of the tidal drag, that is, on D; It is determined by p and e alone.

Capture probabilities into the pth Mercury resonance calculated by Goldreich & Peale (1968) for $e = 0.2$ and Q independent of frequency are shown in Table 5.3. The frequency-independent model gives a good explanation for both capture into the $p = +3/2$ resonance and avoidance of the other, higher-order resonances. However, it does not account for the damping of the amplitude of libration. For the case $H(p,e) > 0$, γ librates about $\gamma_0 \approx 0$ with an amplitude $\gamma_{\max}$ obtained by solving Eq. (5.97) for $\dot{\gamma} = 0$. If we ignore the small displacement of γ_0 from zero, we get

$$\frac{1}{4}\omega_0^2 \cos 2\gamma_{\max} \approx -E/C \tag{5.111}$$

and

$$\dot{\gamma}_{\max} \approx \frac{2\dot{E}}{C\omega_0^2 \sin 2\gamma_{\max}}. \tag{5.112}$$

Damping of the amplitude of libration requires that $\dot{E} < 0$. However,

$$\dot{E} = \langle N_s \rangle \dot{\gamma} \tag{5.113}$$

Table 5.3. The probability, P_p, of capture into the pth Mercury resonance for $e = 0.2$.

p	P_p ($1/Q$ ~Constant)	P_p ($1/Q$ ~Frequency)
+5/2	0.03	0.007
+2	0.15	0.016
+3/2	0.73	0.067
+1	1	0

and if $\langle N_s \rangle$ does not depend on $\dot{\gamma}$, then $\langle \dot{\gamma} \rangle = \langle \dot{E} \rangle = 0$ and the librations are undamped.

The second model considered by Goldreich & Peale (1968) allows that the tidal dissipation function is frequency dependent. In this case, they assumed that

$$\langle N_s \rangle = -K' \sum_{h=-\infty}^{\infty} [H(h,e)]^2 \left(\dot{\theta} - hn\right), \tag{5.114}$$

where K' is a positive constant. Near a resonance $\dot{\theta} = pn + \dot{\gamma}$ and we can write

$$\langle N_s \rangle = -K \left(V + \frac{\dot{\gamma}}{n}\right), \tag{5.115}$$

where

$$K = K'n \sum_h [H(h,e)]^2 \tag{5.116}$$

and

$$V = \frac{\sum_h (p-h)\,[H(h,e)]^2}{\sum_h [H(h,e)]^2}. \tag{5.117}$$

The probability of capture into the pth resonance is given by

$$P_p = \frac{4(\omega_0/n)}{\pi V + 2(\omega_0/n)}. \tag{5.118}$$

For the frequency-dependent case, the probabilities depend on the low-amplitude libration frequency (ω_0/n) and the eccentricity e. The probabilities shown in Table 5.3 are low, but they are not negligible and, in this case, the dependence of $\langle N_s \rangle$ on $\dot{\gamma}$ does result in a term in the expression for $\dot{E}$ that is proportional to $\dot{\gamma}^2$. This term does not average to zero and thus the amplitude of libration is damped.

5.6 Forced Librations

For a satellite trapped in a spin–orbit resonance, for example, the synchronous, 1:1 resonance, analysis of the averaged equation of motion with the drag term included shows that any libration about the equilibrium configuration is damped to zero and the satellite then rotates uniformly with its long axis pointing exactly towards the planet on passage through pericentre. However, the full equation of motion contains short-period terms; consequently the rotational motion of the satellite has short-period librations about the equilibrium configuration.

Consider the rotation of a satellite in a reference frame centred on the satellite and rotating with the satellite's mean motion (see Fig. 5.16). The gravitational

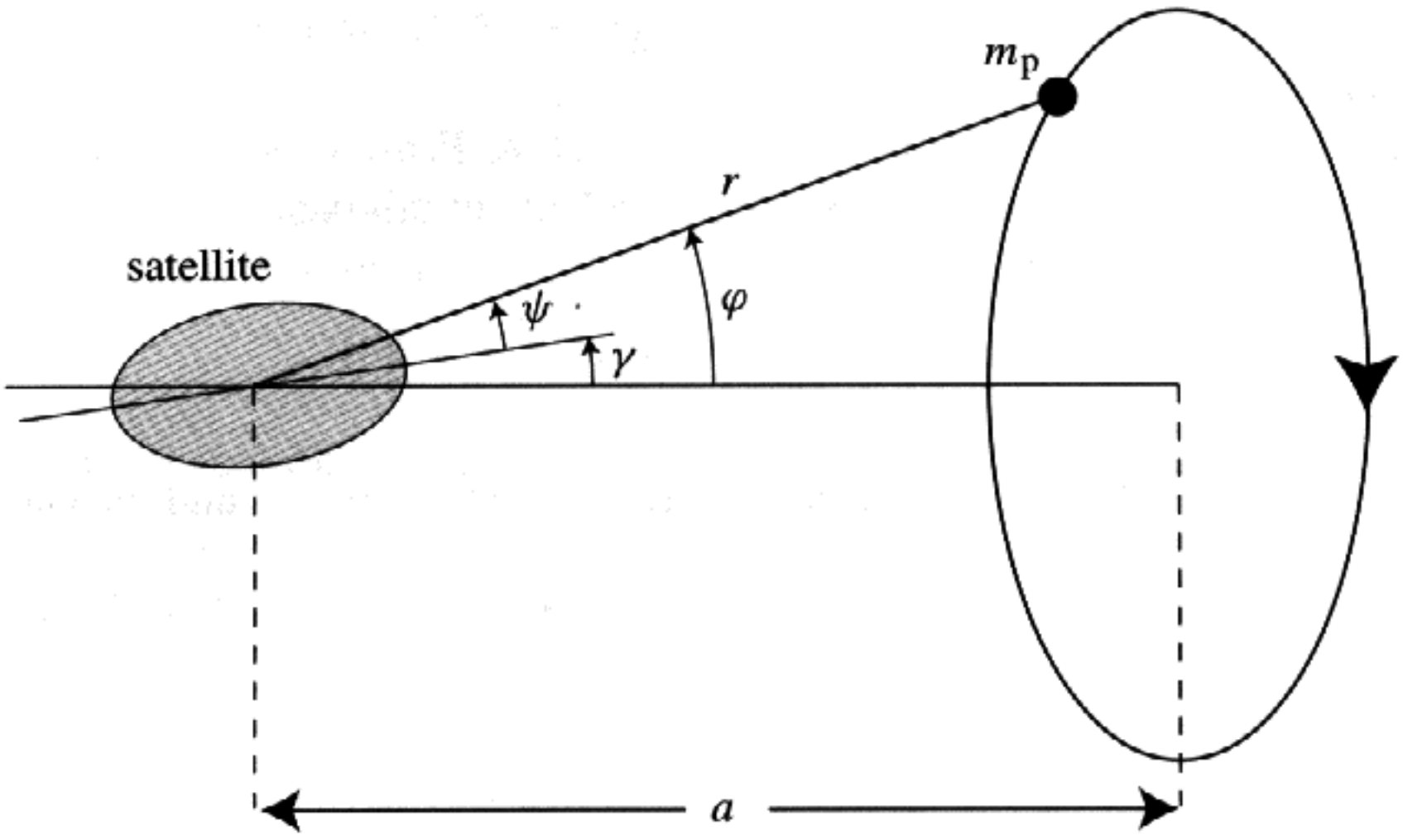

Fig. 5.16. Rotation of a satellite in a rotating reference frame centred on the satellite and rotating with the satellite's mean motion. The planet moves in a 2:1 ellipse about its guiding centre, which, in this frame, is stationary.

torque on the satellite due to the planet is determined by the angle ψ, which in this case is given by

$$\psi = \varphi - \gamma \approx 2e \sin nt - \gamma \tag{5.119}$$

to $\mathcal{O}(e)$, and the full equation of motion, Eq. (5.56), can be written

$$\mathcal{C}\ddot{\gamma} - \frac{3}{2}(\mathcal{B} - \mathcal{A})n^2 \left(\frac{a}{r}\right)^3 \sin(4e \sin nt - 2\gamma) = 0. \tag{5.120}$$

For small deviations from the equilibrium configuration, given that the contribution due to the radial variation in distance r is $(a/r)^3 \approx 1 + 3e \cos nt$, Eq. (5.120) reduces to

$$\mathcal{C}\ddot{\gamma} = -\frac{3}{2}(\mathcal{B} - \mathcal{A})n^2(2\gamma - 4e \sin nt) \tag{5.121}$$

or

$$\ddot{\gamma} = -\omega_0^2 \gamma + 2\omega_0^2 e \sin nt, \tag{5.122}$$

where ω_0 is the libration frequency (see Eq. (5.85)). Substituting $\gamma = \gamma_0 \sin nt$ into this equation and solving for γ_0, the amplitude of the *forced libration,* we obtain

$$\gamma = -\frac{2\omega_0^2 e}{n^2 - \omega_0^2} \sin nt. \tag{5.123}$$

Note that the variation in r does not contribute to this equation. If the forcing frequency n is less than the natural frequency ω_0, then the librations are in phase

with the force. However, if $n > \omega_0$, then the librations and the force are 180° out of phase.

For the Moon, the libration period is 2.86 y while the amplitude of forced libration is ~ 15 arcsec and is too small to detect. However, in the case of Phobos, the highly distorted, innermost satellite of Mars, Duxbury & Callahan (1982) using a control network of ninety-eight craters on forty-three *Viking Orbiter* Phobos pictures obtained a value of 0.8° (±0.2°) for the amplitude of the forced libration. If we assume that the satellite is homogeneous, then the observed value of γ_0 requires that $(\mathcal{B} - \mathcal{A})/\mathcal{C} \approx 0.1$. However, if the satellite is homogeneous, then the observed shape of Phobos implies that $(\mathcal{B} - \mathcal{A})/\mathcal{C} \approx 0.2$. These two widely different values of $(\mathcal{B} - \mathcal{A})/\mathcal{C}$ could be reconciled if the satellite is not homogeneous but has a dense core surrounded by a deep, low-density regolith (Thomas et al. 1986).

5.7 Surface of Section

The method outlined in Sect. 5.4 suggests that, if $\dot{\theta} \approx pn$, we can analyse the motion in the vicinity of a resonance in terms of the slowly varying resonant argument $\gamma = \theta - pM$ using Eq. (5.73). In Fig. 5.17a, we show analytic solutions for the variation of $\dot{\theta}/n$ with θ using values of $\dot{\theta}$ obtained from the energy integral for the motion for γ, which is given by

$$\frac{1}{2}\dot{\gamma}^2 - \frac{1}{4}[\text{sign } H(p, e)]\omega_0^2 \cos 2\gamma = \frac{E_0}{\mathcal{C}}, \tag{5.124}$$

where E_0 is a constant determined by the initial conditions. Analytic solutions are shown for the resonances corresponding to $p = +1/2, +1$, and $+3/2$ and also for the nonresonant case associated with $p = 0$. For the cases corresponding to $p = +1, +3/2$, for which $H(p, e) > 0$, stable equilibrium points exist at $\theta = 0$ and π, whereas for the case corresponding to $p = +1/2$, for which $H(p, e) < 0$, a stable equilibrium point exists at $\theta = \pi/2$. In all cases, for $\dot{\gamma} = 0$ at the stable equilibrium points, we must have

$$E_0 = -\frac{1}{4}\omega_0^2 \mathcal{C} \tag{5.125}$$

and E_0 is a local (remember that ω_0 depends on p) minimum at these points. For values of E_0 in the range

$$-\frac{1}{4}\omega_0^2 \mathcal{C} \leq E_0 < +\frac{1}{4}\omega_0^2 \mathcal{C} \tag{5.126}$$

γ librates about the equilibrium position with an amplitude determined by E_0. The value of E_0 associated with the separatrix that separates regions of libration from those of circulation is given by

$$E_0 = +\frac{1}{4}\omega_0^2 \mathcal{C}. \tag{5.127}$$

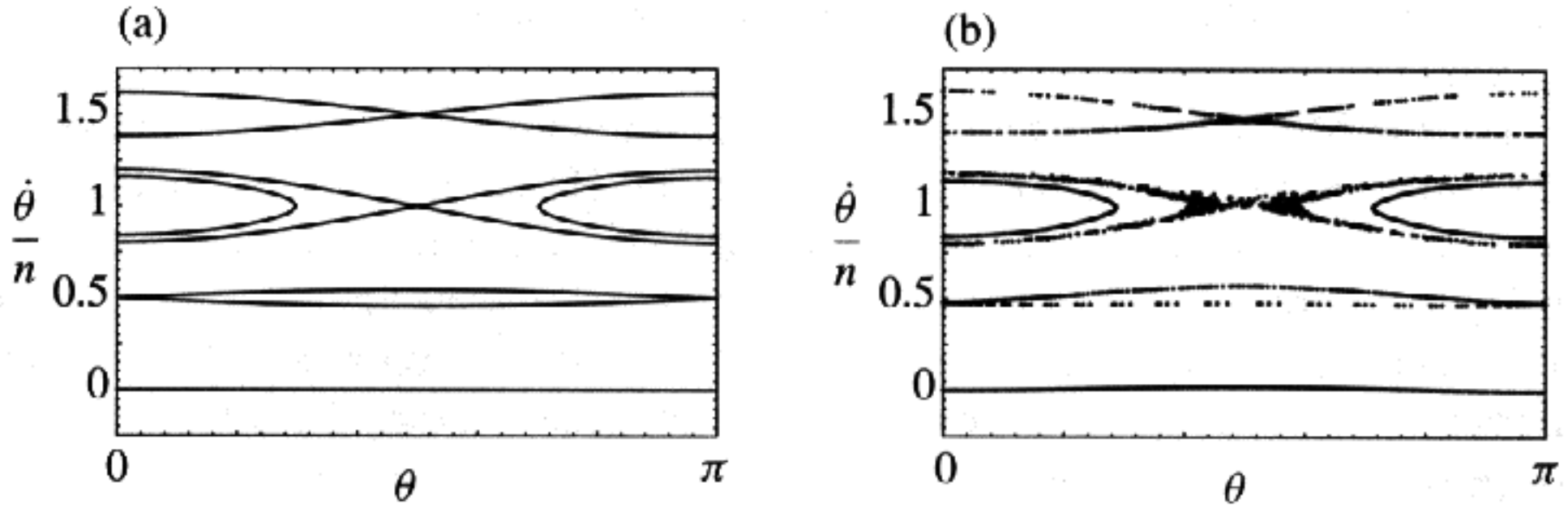

Fig. 5.17. (a) Analytic variation of $\dot{\theta}/n$ with θ on the separatrices of the $p = +1/2$, $+1$, $+3/2$ resonances (and in the libration region of the $p = +1$ resonance) for $\alpha = \sqrt{3(\mathcal{B} - \mathcal{A})/\mathcal{C}} = 0.2$ and $e = 0.1$. (b) A surface of section plot for seven different trajectories in $(\theta, \dot{\theta}/n)$ phase space for the same values of α and e. Values of θ and $\dot{\theta}/n$ are plotted at every passage of the satellite through pericentre.

For motion on the separatrix, the maximum value of $|\dot{\gamma}|$ is given by

$$|\dot{\gamma}_{\max}| = \omega_0 \tag{5.128}$$

and is a measure of the half-width of the resonance. In Fig. 5.17a we show the separatrices associated with various resonances for $e = 0.1$ and $\alpha = (3(\mathcal{B}-\mathcal{A})/\mathcal{C})^{1/2} = 0.2$. Note that, for small amplitudes of libration, the period of libration is $2\pi/\omega_0$, whereas the period of libration on the separatrix is infinite.

To investigate how good an approximation this is, we can integrate the full equation of motion, Eq. (5.56), numerically for fixed values of e and the asphericity parameter α. However, rather than trying to show the full variation of θ and $\dot{\theta}$ with time, we choose to produce a *surface of section* of the motion, which illustrates the fundamental properties of each solution. This involves solving the full equation of motion, Eq. (5.56), numerically and plotting the values of θ and $\dot{\theta}/n$ each time the satellite passes through pericentre. The choice of pericentre is arbitrary, but it is a natural choice in this case because at pericentre $M = 0$ and thus, in this case, the surface of section is equivalent to a plot of γ against $\dot{\gamma}/n$.

In Fig. 5.17b we show surface of section plots for the range of initial conditions $(\theta, \dot{\theta}/n)$ corresponding to the values of $E_0/\mathcal{C}$ used to plot the analytic curves shown in Fig. 5.17a. In both cases, we use $e = 0.1$ and $\alpha = 0.2$. These large values of e and α help to illustrate the sizes of the resonant regions. However, the resonant half-widths are large. For example, in the case of the $p = +1$ resonance, we have $\omega_0 = 0.2$ and it is questionable whether analytic solutions with large amplitudes of libration satisfy our requirement that they are in the "vicinity" of the resonance and that $\dot{\theta} \approx pn$. The surface-of-section method allows us to test the limitations of our analytical theory.

Numerical experiments show that in the heart of each resonant region, close to a stable equilibrium point where the amplitude of libration of θ is small, the

surface of section trajectories in $(\theta, \dot{\theta}/n)$ space mimic the analytic curves with the exception that there is a displacement associated with the forced libration. For example, for the $p = +1$ resonance there is a contribution to $\dot{\gamma}/n$ from the forced libration of -0.0083 (see Eq. (5.115)). This small negative displacement is just about visible in Fig. 5.17b, as are the small positive displacements associated with the $p = +1/2$ and $p = +3/2$ resonances (the displacements are more obvious in Fig. 5.18b where we use even larger values of e and α). For small amplitudes of libration, successive points on the surface-of-section trajectory follow each other in a regular sequence, completing a closed path in a time given by the libration period. However, it is clear from Fig. 5.17b that motion at the separatrix has an additional property. This is particularly evident around the strong $p = +1$ resonance. Motion on the separatrix in our full integration is *chaotic* in the sense that although the evolution of θ follows deterministic laws, it is nevertheless unpredictable and wanders within some finite limits. This accounts for the "fuzzy" appearance of the separatrix trajectory at the $p = +1$ and the $p = +3/2$ resonances.

The trajectories shown in Fig. 5.17b are in very good agreement with the analytic curves shown in Fig. 5.17a, despite the fact that our analysis assumes that we can investigate each resonance in isolation and that the averaged effect of all the other resonances and forced librations is zero. However, it is obvious that as the half-widths of the resonances increase, we must reach a point where this assumption breaks down. In Fig. 5.18a, we show analytic solutions for the motion of θ for the case $e = 0.15$ and $\alpha = 0.3$. In this case, the curves associated with the $p = +1$ and the $p = +3/2$ separatrices overlap close to $\theta = 0$ and $\theta = \pi$, suggesting simultaneous libration in two spin–orbit states,

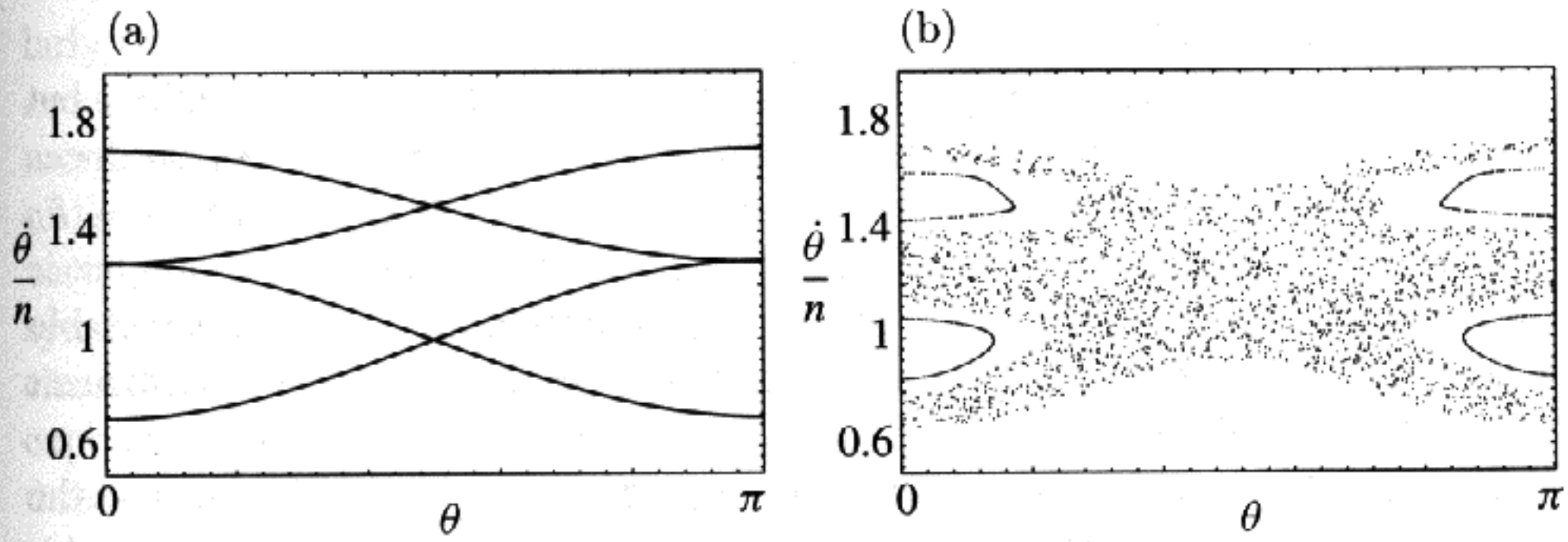

Fig. 5.18. (a) Analytic variation of $\dot{\theta}/n$ with θ on the separatrices and in the libration regions of the $p = +1, +3/2$ resonances for $\alpha = \sqrt{3(B - A)/C} = 0.3$ and $e = 0.15$. (b) A surface of section plot for three different trajectories in $(\theta, \dot{\theta}/n)$ phase space for the same values of α and e. Values of θ and $\dot{\theta}$ are plotted at every passage of the satellite through pericentre.

which is impossible. Chirikov's resonance overlap criterion states that when the sum of the two unperturbed half-widths equals the separation of the resonance centres, large-scale chaos ensues (Chirikov 1979). In the spin–orbit problem, the resonance overlap criterion for the two strongest resonances, the $p = +1$ and the $p = +3/2$, can be written

$$\omega_{0(p=+1)} + \omega_{0(p=+3/2)} \geq \frac{n}{2}, \tag{5.129}$$

which is satisfied if

$$\alpha \geq \frac{1}{2 + \sqrt{14e}} \tag{5.130}$$

(Wisdom et al. 1984).

Chirikov (1979) also estimated that the half-width of the chaotic separatrix, expressed in terms of the chaotic variations of the energy integral, is given by

$$\frac{\Delta E_0}{E_0} \approx 4\pi\varepsilon\lambda^3 \exp(-\pi\lambda/2), \tag{5.131}$$

where ε is the ratio of the coefficient of the nearest perturbing high-frequency term to the coefficient of the perturbed term and $\lambda\ (= \Delta\Omega/\omega_0)$ is the ratio of the frequency difference, $\Delta\Omega$, between the resonant term and the nearest nonresonant term to the frequency of small-amplitude librations, ω_0. For the synchronous spin–orbit state perturbed by the $p = +3/2$ term, $\varepsilon = H(+3/2, e)/H(+1, e) = 7e/2$ and $\lambda = \Delta\Omega/\omega_0 = n/n\alpha = 1/\alpha$. Hence

$$\frac{\Delta E_0}{E_0} \approx \frac{14\pi e}{\alpha^3} \exp(-\pi/2\alpha) \tag{5.132}$$

(Wisdom et al. 1984).

The width of the chaotic separatrix depends linearly on the eccentricity e but exponentially on the asphericity parameter α, and a small increase in α produces a dramatic increase in the width of the chaotic band. The quantity $\Delta E_0/E_0$ is extremely small for near-spherical bodies like Mercury and the Moon but is of the order of unity for irregular bodies like Hyperion and can be appreciable even for bodies like Mimas that have regular shapes but significant permanent distortions (see Table 5.4).

The chaotic zones associated with the separatrices may have had a role in the evolution of the spin rates and orientations of some satellites (Wisdom 1987a,b). The reduction in the energy integral on resonance encounter that must occur if permanent capture into resonance is to be achieved depends on the particular spin–orbit resonance encountered and on the nature of the tidal dissipation mechanism (see Sect. 5.5). However, capture into resonance will occur as described in Sect. 5.5 only if the energy reduction due to tidal forces that occurs in one

Table 5.4. Resonance half-widths.

Body	$(\mathcal{B}-\mathcal{A})/\mathcal{C}$	e	p	$H(p,e)$	ω_0/n	$\Delta E_0/E_0$	$\Delta E_{\text{tides}}/E_0$
Mercury	0.0001	0.2	+3/2	0.64	0.014		
			+1	0.90	0.016	10^{-33}	10^{-6}
			+1/2	−0.10	0.006		
Moon	0.000228	0.055	+3/2	0.19	0.011		
			+1	0.99	0.026	10^{-21}	10^{-5}
			+1/2	−0.03	0.005		
Hyperion	0.26	0.1	+3/2	0.34	0.515		
			+1	0.97	0.870	1.1	10^{-9}
			+1/2	−0.05	0.198		
Mimas	0.06†	0.02	+3/2	0.07	0.112		
			+1	1.00	0.424	0.28	10^{-6}
			+1/2	−0.01	0.042		

†The value of $(\mathcal{B}-\mathcal{A})/\mathcal{C}$ for Mimas is taken from Dermott & Thomas (1988).

librational cycle is significantly greater than the width of the chaotic separatrix. In this regard, it is useful to compare the energy change

$$\delta E_{\text{tides}} \sim \pi \langle N_{\text{s}} \rangle \sim \pi \frac{3}{2} \frac{k_2}{Q_{\text{s}}} \frac{n^4}{\mathcal{G}} R_{\text{s}}^5 \tag{5.133}$$

with the width of the chaotic separatrix, $2\Delta E_0$. Estimates of these quantities for the synchronous case are shown in Table 5.4. Note the marked contrast between the widths of the chaotic zones associated with Mercury and the Moon and those associated with Hyperion and Mimas.

Wisdom (1987a,b) has shown that the synchronous states of all small irregularly shaped satellites in the solar system, even some such as Deimos ($\alpha = 0.8$, $e = 0.0005$) with near-circular orbits, have significant chaotic zones. Furthermore, analysis by Wisdom et al. (1984) and Wisdom (1987a,b) of the stability of the spin axis orientation (we assume in this chapter that the spin axis is always perpendicular to the orbital plane) has shown that the chaotic zone of the synchronous state is attitude unstable. While the satellite is in the synchronous chaotic zone, the slightest deviation of the spin axis from the orbit normal grows exponentially on a very short timescale and the satellite tumbles chaotically in three-dimensional space. All synchronously rotating satellites in the solar system with irregular shapes may have spent a period of time comparable to the tidal despinning time tumbling chaotically before the spin evolved out of the chaotic zone. Wisdom (1987a,b) has speculated on some of the possible geophysical consequences of a prolonged period of tumbling. Of particular interest is the fact that the tumbling state would have involved a significant enhancement in the rate of tidal dissipation as compared to that in the regular synchronous

state. This is because the amplitude of the variation of the tidal distortion in the tumbling state is a factor $1/e$ greater than that in the regular synchronous state (see Sect. 4.10) and the rate of tidal heating of the satellite is increased by a factor $1/e^2$ while the eccentricity damping timescale is decreased by the same factor. Wisdom (1987a,b) has given an interesting discussion of the possible role of chaotic tumbling in the heating of Miranda and the damping of the orbital eccentricity of Deimos.

Exercise Questions

5.1 Where necessary use the data in Appendix A to answer the following questions. (a) Estimate $a - c$ for Jupiter's satellite Io, due to the combined effects of rotation and tidal distortion. (Give your answer in kilometres, and in fractions of the mean radius; assume uniform density.) (b) Repeat part (a) for the Earth's moon, in its current orbit. (c) At an early stage in the history of the Earth–Moon system, the Moon was probably at a distance of only 10 Earth radii, while the Earth's rotation period was about 10 h. Estimate the oblateness, ϵ, and J_2 of the Earth at this time, as well as $a - c$ for the Moon. (d) Mercury rotates with a period of 56 days, or 2/3 of its orbital period of 88 days. Calculate its hydrostatic oblateness, assuming a Love number $k_2 = 3/2$. Do you think ϵ is detectable by current techniques of measurement? Is there any other practicable way to obtain an estimate of the planet's moment of inertia? (e) Both Pluto and its moon Charon are believed to be in states of synchronous rotation. Estimate $a - c$ for each object, assuming that they have equal densities. (You will have to estimate the density first, from Kepler's third law.)

5.2 The current semi-major axis of Charon's orbit is 19,636 km, while the orbital period (and Pluto's spin period) is 6.3872 days. The radius of Pluto is $\sim 1{,}137$ km and that of Charon approximately 600 km. Charon is assumed to be synchronously rotating also, so that the system has reached a stable end point of tidal evolution. (a) Calculate the total mass of the system and the average density of the two bodies. What measurements would be necessary to ascertain the individual masses and densities of Pluto and Charon? (b) Show that the time taken by tides in Pluto to synchronize its spin is

$$\tau_{\rm P} = \frac{2\gamma_{\rm P} Q_{\rm P}}{3\,(k_2)_P} \frac{m_{\rm P}(m_{\rm P} + m_{\rm C})}{m_{\rm C}^2} \left(\frac{a}{R_{\rm P}}\right)^3 \frac{\omega_{\rm P}}{n^2},$$

where $\gamma = C/mR^2$, the initial spin period of Pluto is $2\pi/\omega_{\rm P}$, and the subscripts P and C refer to Pluto and Charon respectively. Estimate $\tau_{\rm P}$, assuming reasonable values for the unknown physical parameters Q, γ, and k_2, and $2\pi/\omega_{\rm P} = 10$ h. (c) Write down (by inspection) the analogous expression for Charon's despinning timescale, $\tau_{\rm C}$, and show that $\tau_{\rm C}/\tau_{\rm P} \approx (R_{\rm C}/R_{\rm P})^6 = 1/50$. (d) What was the initial

semi-major axis of the system and the corresponding orbital period if both Pluto and Charon started with spin periods of 10 h?

5.3 Show from first principles that the approximate potential, V, experienced at a point P at a distance r from the centre of mass, O, of a body of mass m is given by MacCullagh's formula,

$$V = -\frac{\mathcal{G}m}{r} - \frac{\mathcal{G}(\mathcal{A}+\mathcal{B}+\mathcal{C}-3I)}{2r^3},$$

where $\mathcal{A}$, $\mathcal{B}$, and $\mathcal{C}$ are the principal moments of inertia of the body defined with respect to O, and I is the moment of inertia of the body along the line from O to P.

5.4 Consider the rotation of a satellite as it moves in an equatorial orbit around a planet. Let the satellite's orbital radius, semi-major axis, eccentricity, mean anomaly, and true anomaly be r, a, e, M, and f, respectively. An analytical approach to the study of spin–orbit resonance, where the spin rate is approximately p times the mean motion, requires averaging the expression $(a/r)^3 \sin(2\gamma + 2pM - 2f)$ over one orbital period (see Sect. 5.4); here γ is an orientation angle. Use the fourth-order expansions of $(a/r)^3$, $\cos f$, and $\sin f$ given in Sect. 2.5 to derive expressions (to fourth-order in the eccentricity e) for the quantities S_1, S_2, S_3, and S_4 in the equation

$$\left(\frac{a}{r}\right)^3 \sin(2\gamma + 2pM - 2f) = (S_1 + S_2)\sin 2\gamma + (S_3 - S_4)\cos 2\gamma.$$

By finding the time-averaged values, $\langle S_i \rangle = (1/2\pi)\int_0^{2\pi} S_i \, \mathrm{d}M$, show that

$$\left\langle \left(\frac{a}{r}\right)^3 \sin(2\gamma + 2pM - 2f) \right\rangle = H(p,e)\sin 2\gamma$$

and verify the expressions for $H(p,e)$ given in Eqs. (5.74)–(5.82). Given that $H(p,e)$ is related to the strength of a spin–orbit resonance, find the smallest value of e for which the $p = 1$ resonance is weaker than the $p = 3/2$ resonance.

5.5 The long axis of a small, ellipsoidal satellite makes an angle θ with the pericentre direction of its orbit. The differential equation describing the evolution of θ is

$$\mathcal{C}\ddot{\theta} - \frac{3}{2}(\mathcal{B}-\mathcal{A})\frac{\mathcal{G}m_\mathrm{p}}{r^3}\sin 2\psi = 0,$$

where $\mathcal{A}$, $\mathcal{B}$, and $\mathcal{C}$ are the (constant) moments of inertia about the different axes, m_p is the mass of the planet, r is the radial distance of the satellite from the planet, and $\psi = f - \theta$ where f is the true anomaly of the satellite in its orbit. Theoretically, the maximum variation in θ for a satellite trapped in the 1:1 spin–orbit resonance is $\pm 90°$ (see Fig. 5.17a). However, the effect of other resonances reduces this amplitude. Assuming that the satellite is on a fixed orbit such that r

can be found at any time by solving Kepler's equation, write a computer program to solve this differential equation. Taking $(3(\mathcal{B}-\mathcal{A})/\mathcal{C})^{1/2} = 0.25$ and $e = 0.2$, start the satellite at its pericentre with $\theta = 0$. Use different initial values of $\dot{\theta}/n$ (where n is the satellite's mean motion) to determine the maximum variation of θ in the 1:1 spin–orbit resonance.

5.6 Use the analytical theory given in Sect. 5.7 to derive an expression for the minimum and maximum values of $\dot{\theta}/n$ on a surface of section for the retrograde rotation of a satellite trapped in the $p = -1/2$ and the $p = -1$ spin–orbit resonances. If the eccentricity e of the satellite's orbit is fixed, derive an expression for the value of $\alpha = (3(\mathcal{B}-\mathcal{A})/\mathcal{C})^{1/2}$ at which you expect the libration "islands" from these two resonances to intersect. Similarly, if α is fixed, derive an expression for the value of e at which intersection occurs. Use the program written for Question 5.5 to produce a surface of section for $\alpha = 0.25$ and $e = 0.15$ showing clear examples of libration, circulation, and motion near the separatrix for the $p = -1/2$ and $p = -1$ spin–orbit resonances.